

# OODROBUSTBENCH: BENCHMARKING AND ANALYZING ADVERSARIAL ROBUSTNESS UNDER DISTRIBUTION SHIFT

Lin Li<sup>1</sup>, Yifei Wang<sup>2</sup>, Chawin Sitawarin<sup>3</sup> & Michael Spratling<sup>1</sup>

<sup>1</sup>King’s College London, <sup>2</sup>Peking University, <sup>3</sup>UC Berkeley  
 {lin.3.li, michael.spratling}@kcl.ac.uk  
 yifei.wang@pku.edu.cn, chawins@berkeley.edu

## ABSTRACT

Existing works have made great progress in improving adversarial robustness, but typically test their method only on data from the same distribution as the training data, i.e. in-distribution (ID) testing. As a result, it is unclear how such robustness generalizes under input distribution shifts, i.e. out-of-distribution (OOD) testing. This is a concerning omission as such distribution shifts are unavoidable when methods are deployed in the wild. To address this issue we propose a benchmark named OODRobustBench to comprehensively assess OOD adversarial robustness using 23 dataset-wise shifts (i.e. naturalistic shifts in input distribution) and 6 threat-wise shifts (i.e., unforeseen adversarial threat models). OODRobustBench is used to assess 706 robust models using 60.7K adversarial evaluations. This large-scale analysis shows that: 1) adversarial robustness suffers from a severe OOD generalization issue; 2) ID robustness correlates strongly with OOD robustness, in a positive linear way, under many distribution shifts. The latter enables the prediction of OOD robustness from ID robustness. Based on this, we are able to predict the upper limit of OOD robustness for existing robust training schemes. The results suggest that achieving OOD robustness requires designing novel methods beyond the conventional ones. Last, we discover that extra data, data augmentation, advanced model architectures and particular regularization approaches can improve OOD robustness. Noticeably, the discovered training schemes, compared to the baseline, exhibit dramatically higher robustness under threat shift while keeping high ID robustness, demonstrating new promising solutions for robustness against both multi-attack and unforeseen attacks.

## 1 INTRODUCTION

Adversarial attack poses a serious threat to real-world machine learning models, and various approaches have been developed to defend against such attacks. Previous work (Athalye et al., 2018) has shown that adversarial evaluation is critical to the study of adversarial robustness since an unreliable evaluation can often give a false sense of robustness. However, we believe that even state-of-the-art evaluation benchmarks (like RobustBench (Croce et al., 2021)) suffer from a severe limitation: they only consider ID generalization where test data comes from the same distribution as the training data. Since distribution shifts are inevitable in the real world, it is crucial to assess how adversarial robustness is affected when the test distribution differs from the training one.

Although OOD generalization is extensively studied for clean accuracy with rich conclusions (Hendrycks & Dietterich, 2019; Taori et al., 2020; Miller et al., 2021; Baek et al., 2022; Zhao et al., 2022; Yang et al., 2022), there is little known about the OOD generalization of adversarial robustness. To fill this blank, this paper presents for the first time, a comprehensive benchmark, **OODRobustBench**, for assessing out-of-distribution adversarial robustness. Our benchmark is analogous and complementary to RobustBench which is used for assessing in-distribution adversarial robustness. OODRobustBench includes two categories of distribution shift: dataset shift and threat shift (see Fig. 1). Dataset shift denotes test data that has different characteristics from the training data due to varying conditions under which the samples are collected: for images, these

include but are not limited to corruptions, background, and viewpoint. OODRobustBench contains 23 such dataset shifts and assesses adversarial robustness to such data using the attack seen by the model during training. Threat shift denotes a variation between training and test adversarial threat models. In other words, threat shift assesses a model’s robustness to unseen adversarial attacks applied to ID test data. OODRobustBench employs six different types of threat shifts. Adversarial robustness is evaluated for each type of shift to comprehensively assess OOD robustness.

With OODRobustBench, we analyze the OOD generalization behavior of 706 well-trained robust models (a total of 60.7K adversarial evaluations). This model zoo covers a diversity of architectures, robust training methods, data augmentation techniques and training set-ups to ensure the conclusions drawn from this assessment are general and comprehensive. This large-scale analysis reveals that:

- **Adversarial robustness suffers from a severe OOD generalization issue.** Robustness degrades on average by 18%/31%/24% under distribution shifts for CIFAR10  $\ell_\infty$ , CIFAR10  $\ell_2$  and ImageNet  $\ell_\infty$  respectively. Among individual models, the degradation is non-uniform: the higher the ID robustness of the model, the more robustness degrades under distribution shift. Furthermore, an abnormal catastrophic drop in robustness under noise shifts is observed in some methods, e.g., under Gaussian noise shift, the robustness of Rade & Moosavi-Dezfooli (2022) drops by 46% whereas the average drop is just 9%.
- **ID and OOD accuracy/robustness correlate strongly in a linear trend under many shifts** (visualized in Fig. 1). This enables the prediction of OOD performance from ID performance. Furthermore, contrary to the previous finding on standardly-trained (ST) models (Miller et al., 2021), adversarially-trained (AT) models exhibit a much stronger linear correlation between ID and OOD accuracy under most corruption shifts on CIFAR10.
- **Simply following the existing methodology may be insufficient to achieve OOD robustness.** Based on the discovered linear trend, we predict that even the best achievable OOD performance is still far below 100%. For instance, the predicted upper bound of robustness on ImageNet  $\ell_\infty$  is only 43% under the dataset shifts.

Overall, this work reveals that most existing robust models including the state-of-the-art ones are vulnerable to distribution shifts and demonstrates that the existing approaches to improve ID robustness may be insufficient to achieve high OOD robustness. To ensure safe deployment in the wild, we advocate for the assessment of OOD robustness in future models and for the development of new approaches that can cope with distribution shifts better and achieve OOD robustness beyond our prediction.

## 2 RELATED WORK

**Robustness under dataset shift.** Early work (Sehwag et al., 2019) studied the generalization of robustness to novel classes that are unseen during training, e.g., the class of digit “7” in MNIST is novel to the classifier training on CIFAR10. On the other hand, our setup only considers the input distribution shift and not the unforeseen classes. Recently, Sun et al. (2022b) studied the OOD generalization of certified robustness under corruption shifts for a few state-of-the-art methods. In contrast, we focus on empirical robustness instead of certified robustness. Alhamoud et al. (2023) is the most relevant work. They studied the generalization of robustness from multiple source domains to an unseen domain. Different from them, the models we examine are trained on only one source domain, which is the most common set-up in the existing works of adversarial training (Croce et al., 2021). Moreover, we also cover much more diverse distribution shifts, models and training methods than Sun et al. (2022b) and Alhamoud et al. (2023) so that the conclusion drawn in this work is more general and comprehensive. Except for a few exceptions (Geirhos et al., 2020; Sun et al., 2022a; Rusak et al., 2020; Ford et al., 2019), previous work on generalization to input distribution shifts has not considered adversarial robustness. Hence, work on robustness to OOD data and adversarial attacks has generally happened in parallel, as exemplified by RobustBench (Croce et al., 2021) which provides independent benchmarks for assessing performance on corrupt data and adversarial threats.

**Robustness against unforeseen adversarial threat models.** It was observed that naive adversarial training (Madry et al., 2018) with only one single  $\ell_p$  threat model generalizes poorly to unforeseen  $\ell_p$  threat models, e.g., higher perturbation bound (Stutz et al., 2020), different  $p$ -norm (Tramer

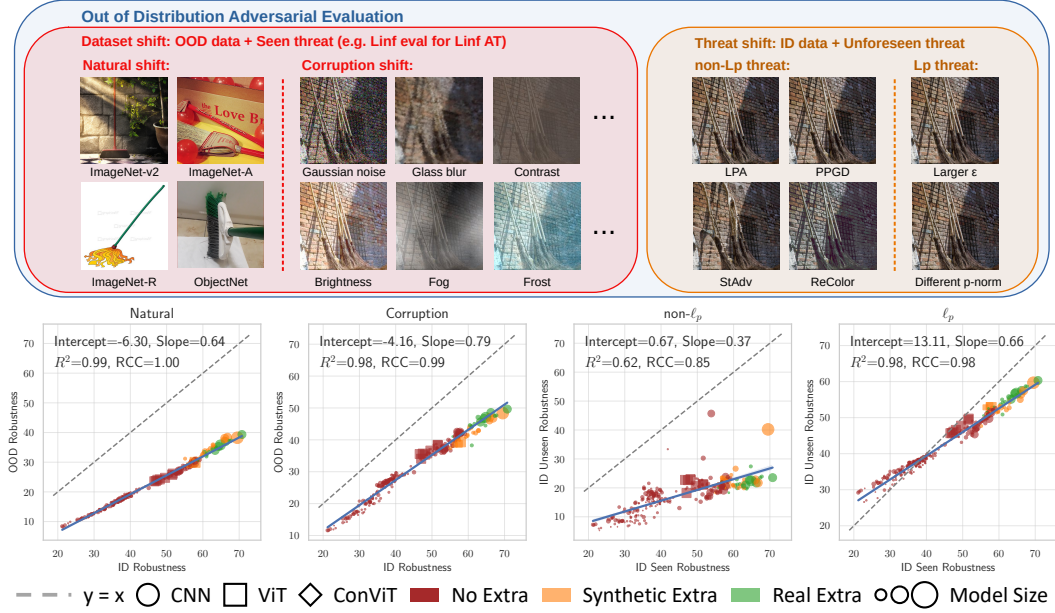


Figure 1: The construction of OODRobustBench (top) and the correlation between ID and OOD robustness under 4 types of distribution shift for CIFAR10  $\ell_\infty$  (bottom). Each marker represents a model and is annotated by its training set-up. The solid blue line is the fitted linear correlation. The dashed gray line ( $y = x$ ) represents perfect generalization where OOD robustness equals ID robustness. Deviation from the dashed line indicates robustness degradation under the respective distribution shift.

& Boneh, 2019; Maini et al., 2020), or non- $\ell_p$  threat models including color transformation ReColor (Laidlaw & Feizi, 2019), spatial transformation StAdv (Xiao et al., 2018), LPIPS-bounded attacks PPdG and LPA (Laidlaw et al., 2021) and many others (Kaufmann et al., 2023). A line of works (Tramer & Boneh, 2019; Maini et al., 2020) defends against a union of  $\ell_p$  threat models by training with multiple  $\ell_p$  threat models jointly, which makes these threat models no longer unforeseen. PAT (Laidlaw et al., 2021) replaces  $\ell_p$  bound with LPIPS (Zhang et al., 2018) in adversarial training and achieves high robustness against several unforeseen attacks. Alternatively, Dai et al. (2022) proposes variation regularization in addition to  $\ell_p$  adversarial training and improves unforeseen robustness. We complement the existing works by conducting a large-scale analysis on the unforeseen robustness of  $\ell_p$  robust models trained by varied methods and training set-ups. We are thus able to provide new insights into the generalization of robustness to unforeseen threat models and identify effective yet previously unknown approaches to enhance unforeseen robustness.

### 3 BENCHMARKING OUT-OF-DISTRIBUTION ADVERSARIAL ROBUSTNESS

This section first proposes the benchmark OODRobustBench and then presents the benchmark results for state-of-the-art robust models.

#### 3.1 OODROBUSTBENCH

OODRobustBench is designed to simulate the possible data distribution shifts that might occur in the wild and evaluate adversarial robustness in the face of them. It focuses on two types of distribution shifts: dataset shift and threat shift. *Dataset shift*,  $OOD_d$ , denotes the distributional difference between training and test raw datasets. *Threat shift*,  $OOD_t$ , denotes the difference between training and evaluation *threat models*, a special type of distribution shift. The original test set drawn from the same distribution as the training set is considered ID. The variant dataset with the same classes yet where the distribution of the inputs differs is considered OOD.

**Dataset shift.** To represent diverse data distribution in the wild, OODRobustBench includes multiple types of dataset shifts from two sources: *natural* and *corruption*. For natural shifts, we adopt four different variant datasets per source dataset: CIFAR10.1 (Recht et al., 2018), CIFAR10.2 (Lu et al., 2020), CINIC (Darlow et al., 2018), and CIFAR10-R (Hendrycks et al., 2021a) for CIFAR10, and ImageNet-v2 (Recht et al., 2019), ImageNet-A (Hendrycks et al., 2021b), ImageNet-R (Hendrycks et al., 2021a), and ObjectNet (Barbu et al., 2019) for ImageNet. For corruption shifts, we adopt, from the corruption benchmarks (Hendrycks & Dietterich, 2019), 15 types of common corruption in four categories: Noise (gaussian, impulse, shot), Blur (motion, defocus, glass, zoom), Weather (fog, snow, frost) and Digital (brightness, contrast, elastic, pixelate, JPEG). Each corruption has five levels of severity. Overall, the dataset-shift testbed consists of 79 ( $4 + 15 \times 5$ ) subsets. App. A.1 describes the details of the above datasets and data processing.

Accuracy and robustness are evaluated on the ID dataset and every OOD dataset. To compute the overall performance of  $\text{OOD}_d$ , we first average the result of natural and corruption shifts:

$$R_c(f) = \mathbb{E}_{i \in \{\text{corruptions}\}, j \in \{\text{severity}\}} R_{i,j}(f) \quad (1)$$

$$R_n(f) = \mathbb{E}_{i \in \{\text{naturals}\}} R_i(f) \quad (2)$$

where  $R(\cdot)$  returns accuracy or adversarial robustness and  $f$  denotes the model to be assessed. Next, we average the above two results to get the overall performance of the dataset shift as

$$R_{ood}(f) = (R_c(f) + R_n(f))/2 \quad (3)$$

**Threat shift.** For  $\ell_p$  AT models, OODRobustBench consists of six unforeseen attacks to simulate threat shifts as in Laidlaw et al. (2021). They are categorized into two groups, non- $\ell_p$  and  $\ell_p$ , according to whether they are bounded by the  $\ell_p$  norm or not.  $\ell_p$  shift includes attacks with the same  $p$ -norm but larger  $\epsilon$  and with different  $p$ -norm. Non- $\ell_p$  shift includes the attacks PPGD, LPA, ReColor, and StAdv. The overall robustness under threat shift,  $\text{OOD}_t$ , is simply the mean of these six unforeseen attacks. App. A.2 describes the specific parameters of these attacks.

### 3.2 OOD PERFORMANCE AND RANKING

The benchmark results for CIFAR10  $\ell_\infty$ ,  $\ell_2$  and ImageNet  $\ell_\infty$  are in Tabs. 1, 2 and 3 respectively.

**Robustness degrades significantly under distribution shift.** For models trained to be robust for CIFAR10  $\ell_\infty$  (Fig. 2), CIFAR10  $\ell_2$  (Fig. 7) and ImageNet  $\ell_\infty$  (Fig. 8), the average drop in robustness (ID adversarial accuracy - OOD adversarial accuracy) is 18%/20%/27% under dataset shift and 18%/42%/22% under threat shift.

Robustness degradation varies greatly across different kinds of shifts. Robustness severely degrades for a subset of shifts: whereas the average robustness degradation of  $\text{OOD}_d$  is 18% on CIFAR10  $\ell_\infty$ , some shifts like CIFAR10-R, fog and contrast degrade by 38%, 30% and 32%, respectively.

Robustness degradation also varies greatly across individual models. As shown in Fig. 2, the distribution of robustness degradation for most shifts spreads over a wide range, suggesting a large variation across individual models. Specifically, we find that the higher the ID robustness of the model, the more robustness degrades under the shifts. For example, the top method in Tab. 1 degrades by 30% of robustness, while the bottom method degrades by only 18%. This suggests that while the great progress has been made on improving ID robustness, we only gain diminishing returns under the distribution shifts.

Catastrophic degradation under noise shifts. We highlight that some methods suffer from abnormally catastrophic degradation in robustness under noise shifts constituting the outliers under noise shifts in Fig. 2. This issue is most severe on Rade & Moosavi-Dezfooli (2022) whose robustness falls by 43%/46%/38% under impulse/Gaussian/shot noise, whereas the average drop is 12%/9%/8% (discussed in App. D). A similar yet milder drop is also observed on Debenedetti et al. (2023) and models trained with some advanced data augmentations like AutoAugment (Cubuk et al., 2019).

**Higher ID robustness generally implies higher OOD robustness but not always.** The ranking of ID and OOD robustness is generally consistent (see the last two columns of Tabs. 1, 2 and 3). However, some of the models do break this trend. In Tab. 1, the ranking of Rade & Moosavi-Dezfooli (2022) drops from 22 to 57 due to catastrophic degradation, while the ranking of Pang et al. (2020) jumps from 70 to 3 due to its superior robustness under threat shift (analyzed in Sec. 5.3).



Table 1: Performance, evaluated with OODRobustBench, of state-of-the-art models trained on CIFAR10 to be robust to  $\ell_\infty$  attacks and corruptions. Top 3 results under each metric are highlighted by **bold** and/or underscore. Severe ranking discrepancies are marked in **red**. The column “OOD” gives the overall OOD robustness which is the mean of the robustness to  $\text{OOD}_d$  and  $\text{OOD}_t$ .

Training Threat	Method	Accuracy (%)		Robustness (%)				Ranking (Rob.)	
		ID	$\text{OOD}_d$	ID	$\text{OOD}_d$	$\text{OOD}_t$	$\text{OOD}$	ID	$\text{OOD}$
$\ell_\infty$	Wang et al. (2023) (WRN-70-16)	93.25	76.04	<b>70.76</b>	<b>44.49</b>	35.80	<b>40.14</b>	1	2
	Bai et al. (2023)	<b>95.23</b>	79.09	<b>69.50</b>	<b>43.32</b>	<b>46.71</b>	<b>45.01</b>	2	1
	Cui et al. (2023)	92.16	74.88	<u>67.77</u>	42.48	35.48	38.98	3	4
	Wang et al. (2023) (WRN28-10)	92.44	75.04	<u>67.34</u>	42.34	35.26	38.80	4	5
	Rebuffi et al. (2021)	92.23	74.89	66.79	<u>42.60</u>	33.65	38.12	5	9
	Gowal et al. (2021b)	88.74	70.68	66.24	42.76	33.65	38.20	6	8
	Gowal et al. (2021a)	91.10	73.24	66.03	42.58	34.00	38.29	7	7
	Huang et al. (2023)	91.58	73.89	65.87	41.70	33.34	37.52	8	12
	Rebuffi et al. (2021)	88.50	70.65	64.82	41.43	33.90	37.66	9	10
	Xu et al. (2022)	93.69	77.22	64.74	39.67	37.02	38.34	10	6
	Schwag et al. (2022)	87.21	69.20	62.72	40.77	32.35	36.56	17	15
	Rade & Moosavi-Dezfooli (2022)	88.16	69.45	60.98	35.10	30.20	32.65	<b>22</b>	<b>57</b>
	Wu et al. (2020)	88.25	69.82	60.14	38.20	31.39	34.80	26	27
	Carmon et al. (2019)	89.69	71.57	59.80	36.74	31.12	33.93	28	38
	Wang et al. (2020)	87.50	70.23	56.75	35.50	32.68	34.09	52	35
	Pang et al. (2020)	85.14	66.96	53.84	32.45	<b>46.20</b>	<u>39.33</u>	<b>70</b>	<b>3</b>
	Zhang et al. (2020)	84.52	65.94	53.65	32.95	31.84	<u>32.40</u>	71	59
	Rice et al. (2020)	85.34	66.46	53.52	32.07	27.89	29.98	72	89
	Zhang et al. (2019)	84.92	66.51	52.68	31.68	26.54	29.11	76	99
	Wong et al. (2020)	83.34	64.96	43.33	25.35	24.82	25.08	111	112
Corruption	Diffenderfer et al. (2021)	<b>96.56</b>	<b>83.54</b>	1.00	0.50	0.00	0.25	261	261
	Kireev et al. (2022)	<u>94.75</u>	<b>80.39</b>	0.16	0.06	0.00	0.03	262	262

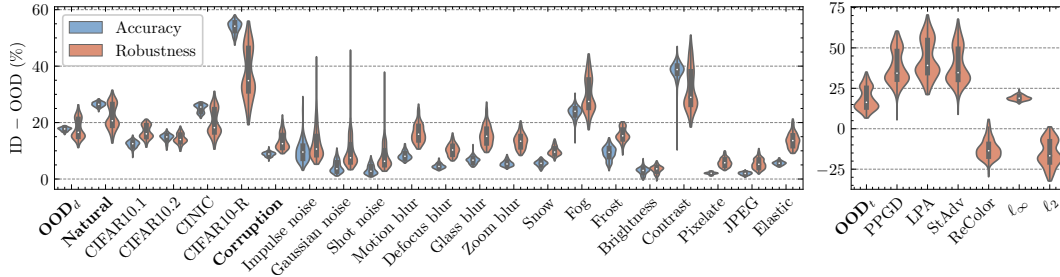


Figure 2: Degradation of accuracy and robustness under various distribution shifts for CIFAR10  $\ell_\infty$ .

#### 4 THE LINEAR TREND BETWEEN ID AND OOD PERFORMANCE

In Sec. 3.2, we have seen that the robustness ranking among the models is generally preserved under the distribution shift. Here, we further show that the ID and OOD adversarial accuracy of existing models are strongly and linearly correlated under many shifts. We also find that adversarial training, compared to standard training, significantly improves the linear correlation between ID and OOD accuracy under most corruption shifts. Based on the discovered linear trend, we predict the upper limit of OOD performance for the existing robust training techniques and observe a large gap between the predicted upper limit and the ideal best OOD robustness, suggesting that novel approaches beyond the existing ones are required to achieve OOD robustness.

The following result is based on a large-scale analysis including over 60K OOD evaluations of 706 models. 187 of these models were retrieved from RobustBench or other published works so as to include current state-of-the-art methods, and the remaining models were trained by ourselves. These models are mainly trained in three set-ups: CIFAR10  $\ell_\infty$ , CIFAR10  $\ell_2$  and ImageNet  $\ell_\infty$ . They cover a wide range of model architectures, model sizes, data augmentation methods, training and regularization techniques. More detail is given in App. B.

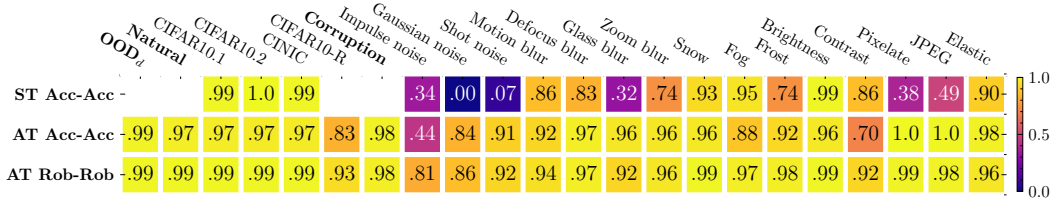


Figure 3:  $R^2$  of regression between ID and OOD performance for Standardly-Trained (ST) and Adversarially-Trained (AT) models under various dataset shifts for CIFAR10  $\ell_\infty$ . Higher  $R^2$  implies stronger linear correlation. The results for ST models were copied from Miller et al. (2021). Some results of ST are missing (blank cells) because they were not reported in Miller et al. (2021).

#### 4.1 DATASET SHIFT

This section studies how ID and OOD accuracy/robustness correlate under dataset shifts. We fit a linear regression on four pairs of metrics (Acc-Acc, Rob-Rob, Acc-Rob, and Rob-Acc) for each dataset shift and each training setup (CIFAR10  $\ell_\infty$ , CIFAR10  $\ell_2$  and ImageNet  $\ell_\infty$ ). Taking Acc-Rob as an example, a linear model is fitted with ID accuracy as the observed variable  $x$  and OOD adversarial robustness as the target variable  $y$ . The result of regression for each shift is given in App. G. Below are the major findings.

**ID accuracy (resp. robustness) strongly correlates with OOD accuracy (resp. robustness) in a linear relationship** for most dataset shifts. Across CIFAR10  $\ell_\infty$  (Fig. 3), CIFAR10  $\ell_2$  (Fig. 9) and ImageNet  $\ell_\infty$  (Fig. 10), the regression of Acc-Acc and Rob-Rob for most shifts achieve very high  $R^2$  ( $> 0.9$ ), i.e., their relationship can be well explained by a linear model. This suggests for these shifts ID performance is a good indication of performance under shift, and more importantly, OOD performance can be reliably predicted by ID performance using the fitted linear model.

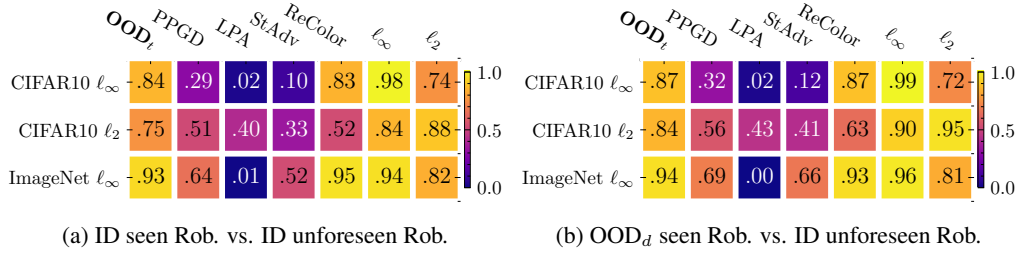
**Nevertheless, under some shifts, ID and OOD performance are only weakly correlated.** Natural shifts like CIFAR10-R and ImageNet-A and corruption shifts like noise, fog and contrast are observed to have relatively low  $R^2$  across varied training set-ups in Figs. 3, 9 and 10. It can be seen from Figs. 15 and 16 that the correlation for these shifts becomes even weaker, and the gap of  $R^2$  between them and the others expands, as more inferior (relatively worse accuracy and/or robustness) models are excluded from the regression. This suggests that the models violating the linear trend are mostly high-performance. App. E discusses how inferior models are identified and how they influence the correlation.

The correlation appears to be less related to the degradation, i.e., model performance may fall greatly under some shifts but still correlate well between ID and OOD or vice versa. For example, noise shifts degrade accuracy/robustness mildly in Fig. 2 but have roughly the weakest correlation, whereas CIFAR10-R degrades the most but has a relatively strong correlation.

**AT models exhibit a stronger linear correlation between ID and OOD accuracy.** This is the case under most corruption shifts on CIFAR10 in Figs. 3 and 9. The improvement is dramatic for particular shifts. For example,  $R^2$  surges from nearly 0 (no linear correlation) for ST models to around 0.8 (evident linear correlation) for AT models with Gaussian and shot noise data shifts. These results are contrary to the previous finding on ST models (Miller et al., 2021). However, note that we measure linear correlation for the raw data, whereas Miller et al. (2021) applies a nonlinear transformation to the data to promote linearity. Overall, adversarial training boosts linear correlation for corruption shifts, and hence, improves the faithfulness of using ID performance for model selection and OOD performance prediction.

We attribute this to AT improving accuracy on the corrupted data (Kireev et al., 2022). Intuitively, ST models have less correlated corruption accuracy because corruption significantly impairs accuracy and such effect varies a lot among models. Compared to ST, AT effectively mitigates the effect of corruption on accuracy, and hence, reduces the divergence of corruption accuracy so that corruption accuracy is more correlated to ID accuracy.

Last, we observe **no evident correlation when ID and OOD metrics misalign, i.e., Acc-Rob and Rob-Acc for CIFAR10**, but weak correlation for ImageNet  $\ell_\infty$  as shown in Fig. 11.

Figure 4:  $R^2$  of regression between seen robustness and unforeseen robustness, i.e., threat shift.

## 4.2 THREAT SHIFT

This section studies the relationship between seen and unforeseen robustness, where seen robustness is computed for both ID and OOD<sub>d</sub> data. Unforeseen robustness is computed only using ID data. Linear regression is then conducted between seen robustness ( $x$ ) and unforeseen robustness ( $y$ ). The result of regression for each threat shift is given in App. H. The sensitivity of the regression results to the composition of the model zoo is discussed in App. E.

**$\ell_p$  robustness correlates weakly with non- $\ell_p$  robustness.** The regression between ID seen (i.e.,  $\ell_p$ ) robustness and unforeseen robustness (i.e., PP GD, LPA and StAdv) consistently produces  $R^2$  below 0.7 across varied training datasets and threat models in Fig. 4a. This means that their relationship cannot be well explained by a linear model. The linear correlation between  $\ell_p$  and ReColor is much more evident for  $\ell_\infty$  AT models but not  $\ell_2$ . Nevertheless,  $\ell_2$  AT models show a significantly stronger correlation with non- $\ell_p$  robustness than  $\ell_\infty$  AT models, except for ReColor. A similar advantage is also observed in ImageNet models when compared to CIFAR10 models.

**$\ell_p$  robustness correlates strongly with  $\ell_p$  robustness of different  $\epsilon$  and  $p$ -norm.**  $R^2$  of their regression is higher than 0.7 across all assessed set-ups in Fig. 4a suggesting a consistently strong linear correlation. The correlation between different  $\epsilon$  of the same  $p$ -norm is stronger than the correlation between different  $p$ -norm. Therefore, ID seen  $\ell_p$  robustness is useful for selecting a model robust to different  $\epsilon$  and  $p$ -norm attacks, as well as predicting the  $\ell_p$  robustness of that model.

**OOD<sub>d</sub> seen robustness correlates more strongly than ID seen robustness with unforeseen robustness.** For non- $\ell_p$  threat shifts, the regression w.r.t. OOD<sub>d</sub> seen robustness (Fig. 4b) consistently has higher  $R^2$  than that of ID seen robustness (Fig. 4a) across all training set-ups. This may imply a deeper underlying relationship between the dataset and the threat shifts.

## 4.3 PREDICTED UPPER LIMIT OF OOD PERFORMANCE

Based on the precise linear trend observed above for existing robust training methods, we can predict the OOD performance of a model trained by such a method from its ID performance using the fitted linear model. Furthermore, we can extrapolate from current trends to predict the maximum OOD robustness that can be expected from a hypothetical future model that achieves perfect robustness on ID data (assuming the linear trend continues).

$$\text{Upper limit of OOD accuracy/robustness (\%)} = \text{slope} * 100 + \text{intercept}. \quad (4)$$

This estimates the best OOD performance one can expect by fully exploiting existing robust training techniques. Note that a wide range of models and techniques (App. B) are covered by our correlation analysis so their, as well as their variants', OOD performance should be (approximately) bounded by the predicted upper limit. The accuracy of the prediction depends on the  $R^2$  of the corresponding correlation.

We find that **continuously improving ID robustness following existing practice may not lead to satisfactory OOD robustness.** The upper limit of OOD robustness under dataset shift, OOD<sub>d</sub>, is 66%/71%/43% for CIFAR10  $\ell_\infty$  (Fig. 5), CIFAR10  $\ell_2$  (Fig. 13) and ImageNet  $\ell_\infty$  (Fig. 14) respectively, and under threat shift OOD<sub>t</sub> is 52%/35%/52% correspondingly. Hence, if current trends continue, the resulting models are likely to be very unreliable in real-world applications. The vulnerability of models is most evident for ImageNet  $\ell_\infty$  under dataset shift and for CIFAR10  $\ell_2$

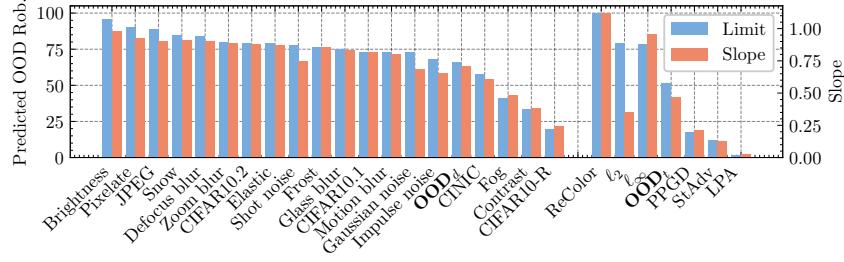


Figure 5: The estimated upper limit of OOD robustness and the conversion rate, a.k.a. slope, to OOD robustness from ID robustness under various distribution shifts for CIFAR10  $\ell_\infty$ . The estimated upper limit is capped by 100% as robustness can not surpass 100%.

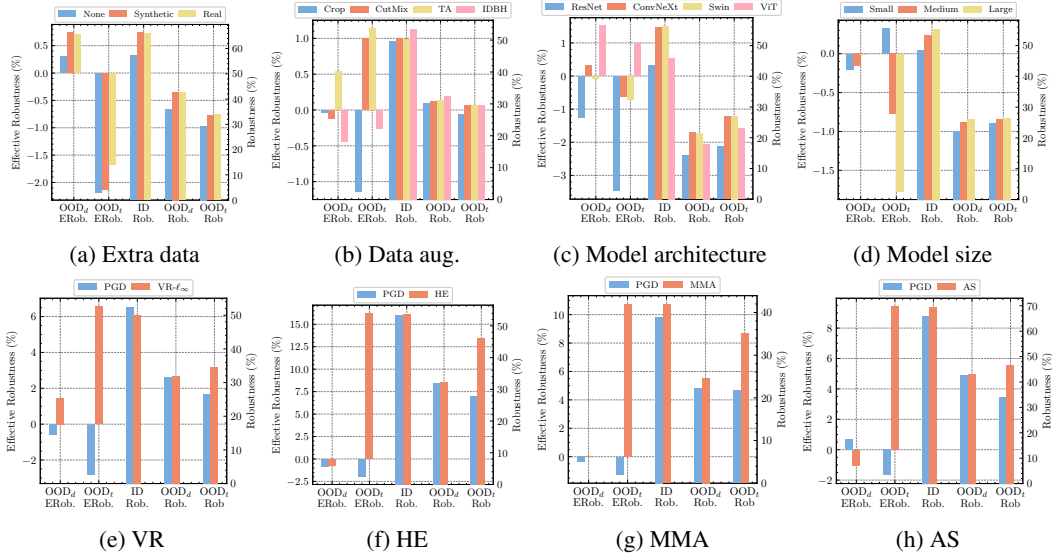


Figure 6: The robustness (Rob.) and effective robustness (ERob.) of robust training techniques.

under threat shift. The expected upper limit of OOD robustness also varies greatly among individual shifts ranging from nearly 0 to 100%.

One of the accounts for this issue is that the existing methods have poor conversion rate to OOD robustness from ID robustness as shown by the slope of the linear trend in Figs. 5, 13 and 14. Taking an example of fog shift on ImageNet, the slope is roughly 0.1 so improving 10% ID robustness can only lead to 1% improvement on fog robustness. Besides, the upper limit and conversion rate of robustness are observed to be much lower than those of accuracy in Figs. 12 to 14, suggesting the OOD generalization issue is more severe for robustness. Overall, this issue calls for developing novel methods that can improve OOD robustness beyond our prediction.

## 5 IMPROVING OOD GENERALIZATION OF ROBUSTNESS

To inspire the design of methods that have OOD robustness exceeding the above prediction, this section investigates methods that have the potential to be effective for boosting the OOD generalization of robustness. The effectiveness is quantified by two metrics: OOD performance and effective performance. Effective performance measures the extra resilience of a model under distribution shift when compared to a group of models by adapting the metric of “Effective Robustness” Taori et al. (2020):

$$R'(f) = R_{ood}(f) - \beta(R_{id}(f)) \quad (5)$$

where  $\beta(\cdot)$  is a linear mapping from ID to OOD metric fitted on a group of models. Different from Taori et al. (2020), we name this metric effective accuracy (robustness) when  $R_{id}$  and  $R_{ood}$  are accuracy (robustness). A positive effective robustness means that  $f$  achieves adversarial robustness above what the linear trend predicts based on its ID performance, i.e.,  $f$  is advantageous over the fitted models on OOD generalization. Note that higher effective robustness is not equivalent to higher OOD robustness since the model may have a lower ID robustness.

The specific set-ups and detailed results of the following experiments are described in App. F.

### 5.1 DATA

**Training with extra data** boosts both robustness and effective robustness for both dataset and threat shifts compared to training schemes without extra data (see Fig. 6a). The improved effective robustness suggests that this technique induces extra OOD generalizability. There is no clear advantage to training with extra real data (Carmon et al., 2019) rather than synthetic data (Gowal et al., 2021b) except for the effective robustness under threat shift which is improved more by real data.

**Advanced data augmentation** improves robustness under both types of shifts and effective robustness under threat shift over the baseline augmentation RandomCrop (see Fig. 6b). Nevertheless, advanced data augmentation methods other than TA (Müller & Hutter, 2021) degrade effective robustness under dataset shift. TA has inferior ID and OOD robustness than IDBH but consistently achieves the highest effective robustness.

### 5.2 MODEL

**Advanced model architecture** significantly boosts robustness and effective robustness under both types of shift over the classical architecture ResNet (He et al., 2016) (Fig. 6c). ConvNeXt (Liu et al., 2022) and Swin (Liu et al., 2021) achieve the highest OOD robustness mainly due to their high ID robustness. Among all tested architectures, ViT (Dosovitskiy et al., 2021) achieves the highest effective robustness.

**Scaling model up** improves robustness under both types of shift and effective robustness under dataset shift, but dramatically impairs effective robustness under threat shift (Fig. 6d). The latter is because increasing model size greatly improves ID robustness but not OOD robustness so that the real OOD robustness is much below the OOD robustness predicted by linear correlation.

### 5.3 TRAINING

**VR** (Dai et al., 2022), the state-of-the-art defense against unforeseen attacks, greatly boosts effective robustness under threat shifts so that it achieves higher OOD robustness than the baseline in spite of inferior ID robustness. Surprisingly, VR also clearly boosts effective robustness under dataset shift even though not designed for dealing with these shifts.

Training methods **HS** (Pang et al., 2020), **MMA** (Ding et al., 2020) and **AS** (Bai et al., 2023) achieve an effective robustness of 16.22%, 10.74% and 9.41%, respectively, under threat shift, which are much higher than corresponding models trained with PGD. Importantly, in contrast to VR, these methods also improve ID robustness resulting in a further boost on OOD robustness. This makes them a potentially promising defense against multi-attack (Dai et al., 2023).

## 6 CONCLUSIONS

This work proposes a new benchmark to assess OOD adversarial robustness, provides many insights into the generalization of existing robust models under distribution shift and identifies several robust interventions beneficial to OOD generalization. We have analyzed the OOD robustness of hundreds of diverse models to ensure that we obtain generally applicable insights. As we focus on general trends, our analysis does not provide a detailed investigation into individual methods or explain the observed outliers such as the catastrophic robustness degradation. However, OODRobustBench provides a tool for performing such more detailed investigations in the future. It also provides a means of measuring progress towards models that are more robust in real-world conditions and will, hopefully, spur the future development of such models.

## REFERENCES

- Kumail Alhamoud, Hasan Abed Al Kader Hammoud, Motasem Alfarra, and Bernard Ghanem. Generalizability of Adversarial Robustness Under Distribution Shifts. *Transactions on Machine Learning Research*, May 2023. ISSN 2835-8856. URL [https://openreview.net/forum?id=XNfo3dQiCJ&referrer=%5BTMLR%5D\(%2Fgroup%3Fid%3DTMLR\)](https://openreview.net/forum?id=XNfo3dQiCJ&referrer=%5BTMLR%5D(%2Fgroup%3Fid%3DTMLR)).
- Anish Athalye, Nicholas Carlini, and David Wagner. Obfuscated Gradients Give a False Sense of Security: Circumventing Defenses to Adversarial Examples. In *Proceedings of the 35th International Conference on Machine Learning*, pp. 274–283. PMLR, July 2018. URL <https://proceedings.mlr.press/v80/athalye18a.html>. ISSN: 2640-3498.
- Maximilian Augustin, Alexander Meinke, and Matthias Hein. Adversarial robustness on in-and out-distribution improves explainability. In *European Conference on Computer Vision*, pp. 228–245. Springer, 2020.
- Christina Baek, Yiding Jiang, Aditi Raghunathan, and J Zico Kolter. Agreement-on-the-line: Predicting the performance of neural networks under distribution shift. In *Advances in Neural Information Processing Systems*, volume 35, pp. 19274–19289, 2022.
- Yatong Bai, Brendon G. Anderson, Aerin Kim, and Somayeh Sojoudi. Improving the Accuracy-Robustness Trade-Off of Classifiers via Adaptive Smoothing, May 2023. URL <http://arxiv.org/abs/2301.12554>. arXiv:2301.12554 [cs].
- Andrei Barbu, David Mayo, Julian Alverio, William Luo, Christopher Wang, Dan Gutfreund, Josh Tenenbaum, and Boris Katz. ObjectNet: A large-scale bias-controlled dataset for pushing the limits of object recognition models. In *Advances in Neural Information Processing Systems*, volume 32. Curran Associates, Inc., 2019. URL <https://proceedings.neurips.cc/paper/2019/hash/97af07a14cacba681feacf3012730892-Abstract.html>.
- Yair Carmon, Aditi Raghunathan, Ludwig Schmidt, John C Duchi, and Percy S Liang. Unlabeled Data Improves Adversarial Robustness. In *Advances in Neural Information Processing Systems*, pp. 12, 2019.
- Francesco Croce and Matthias Hein. Reliable Evaluation of Adversarial Robustness with an Ensemble of Diverse Parameter-free Attacks. In *Proceedings of the 37th International Conference on Machine Learning*, pp. 11, 2020.
- Francesco Croce, Maksym Andriushchenko, Vikash Sehwal, Edoardo Debenedetti, Nicolas Flammarion, Mung Chiang, Prateek Mittal, and Matthias Hein. RobustBench: a standardized adversarial robustness benchmark. In *Thirty-fifth Conference on Neural Information Processing Systems Datasets and Benchmarks Track (Round 2)*, October 2021. URL <https://openreview.net/forum?id=SSKZPJct7B>.
- Ekin D. Cubuk, Barret Zoph, Dandelion Mane, Vijay Vasudevan, and Quoc V. Le. AutoAugment: Learning Augmentation Strategies From Data. In *2019 IEEE/CVF Conference on Computer Vision and Pattern Recognition (CVPR)*, pp. 113–123, Long Beach, CA, USA, June 2019. IEEE. ISBN 978-1-72813-293-8. doi: 10.1109/CVPR.2019.00020. URL <https://ieeexplore.ieee.org/document/8953317/>.
- Jiequan Cui, Zhuotao Tian, Zhisheng Zhong, Xiaojuan Qi, Bei Yu, and Hanwang Zhang. Decoupled Kullback-Leibler Divergence Loss, May 2023. URL <http://arxiv.org/abs/2305.13948>. arXiv:2305.13948 [cs].
- Sihui Dai, Saeed Mahloujifar, and Prateek Mittal. Formulating Robustness Against Unforeseen Attacks. In *Advances in Neural Information Processing Systems*, volume 35, pp. 8647–8661, December 2022. URL [https://proceedings.neurips.cc/paper\\_files/paper/2022/hash/392ac56724c133c37d5ea746e52f921f-Abstract-Conference.html](https://proceedings.neurips.cc/paper_files/paper/2022/hash/392ac56724c133c37d5ea746e52f921f-Abstract-Conference.html).
- Sihui Dai, Saeed Mahloujifar, Chong Xiang, Vikash Sehwal, Pin-Yu Chen, and Prateek Mittal. MultiRobustBench: Benchmarking Robustness Against Multiple Attacks, May 2023. URL <http://arxiv.org/abs/2302.10980>. arXiv:2302.10980 [cs].

- Luke N. Darlow, Elliot J. Crowley, Antreas Antoniou, and Amos J. Storkey. CINIC-10 is not ImageNet or CIFAR-10, October 2018. URL <http://arxiv.org/abs/1810.03505>. arXiv:1810.03505 [cs, stat].
- Edoardo Debenedetti, Vikash Sehwal, and Prateek Mittal. A Light Recipe to Train Robust Vision Transformers. In *First IEEE Conference on Secure and Trustworthy Machine Learning*, February 2023. URL <https://openreview.net/forum?id=IztT98ky0cKs>.
- James Diffenderfer, Brian Bartoldson, Shreya Chaganti, Jize Zhang, and Bhavya Kailkhura. A Winning Hand: Compressing Deep Networks Can Improve Out-of-Distribution Robustness. In *Advances in Neural Information Processing Systems*, volume 34, pp. 664–676. Curran Associates, Inc., 2021. URL <https://proceedings.neurips.cc/paper/2021/hash/0607f4c705595b911a4f3e7a127b44e0-Abstract.html>.
- Gavin Weiguang Ding, Yash Sharma, Kry Yik Chau Lui, and Ruitong Huang. MMA Training: Direct Input Space Margin Maximization through Adversarial Training. In *International Conference on Learning Representations*, 2020. URL <https://openreview.net/forum?id=HkeryxBtPB>.
- Alexey Dosovitskiy, Lucas Beyer, Alexander Kolesnikov, Dirk Weissenborn, Xiaohua Zhai, Thomas Unterthiner, Mostafa Dehghani, Matthias Minderer, Georg Heigold, Sylvain Gelly, Jakob Uszkoreit, and Neil Houlsby. An Image is Worth 16x16 Words: Transformers for Image Recognition at Scale. In *International Conference on Learning Representations*, 2021. URL [https://openreview.net/forum?id=YicbFdNTTy&utm\\_campaign=f86497ed3a-EMAIL\\_CAMPAIGN\\_2019\\_04\\_24\\_03\\_18\\_COPY\\_01&utm\\_medium=email&utm\\_source=Deep%20Learning%20Weekly&utm\\_term=0\\_384567b42d-f86497ed3a-72965345](https://openreview.net/forum?id=YicbFdNTTy&utm_campaign=f86497ed3a-EMAIL_CAMPAIGN_2019_04_24_03_18_COPY_01&utm_medium=email&utm_source=Deep%20Learning%20Weekly&utm_term=0_384567b42d-f86497ed3a-72965345).
- Logan Engstrom, Andrew Ilyas, Hadi Salman, Shibani Santurkar, and Dimitris Tsipras. Robustness (python library), 2019. URL <https://github.com/MadryLab/robustness>.
- Nic Ford, Justin Gilmer, Nicolas Carlini, and Dogus Cubuk. Adversarial examples are a natural consequence of test error in noise. 2019. doi: 10.48550/arXiv.1901.10513.
- Ruize Gao, Jiong Xiao Wang, Kaiwen Zhou, Feng Liu, Binghui Xie, Gang Niu, Bo Han, and James Cheng. Fast and Reliable Evaluation of Adversarial Robustness with Minimum-Margin Attack. In *Proceedings of the 39th International Conference on Machine Learning*, pp. 7144–7163. PMLR, June 2022. URL <https://proceedings.mlr.press/v162/gao22i.html>. ISSN: 2640-3498.
- Robert Geirhos, Jörn-Henrik Jacobsen, Claudio Michaelis, Richard Zemel, Wieland Brendel, Matthias Bethge, and Felix A. Wichmann. Shortcut learning in deep neural networks. *Nature Machine Intelligence*, 2(11):665–73, 2020. doi: 10.1038/s42256-020-00257-z.
- Sven Gowal, Chongli Qin, Jonathan Uesato, Timothy Mann, and Pushmeet Kohli. Uncovering the Limits of Adversarial Training against Norm-Bounded Adversarial Examples. arXiv:2010.03593 [cs, stat], March 2021a. URL <http://arxiv.org/abs/2010.03593>. arXiv: 2010.03593.
- Sven Gowal, Sylvestre-Alvise Rebuffi, Olivia Wiles, Florian Stimberg, Dan Calian, and Timothy Mann. Improving Robustness using Generated Data. In *Thirty-Fifth Conference on Neural Information Processing Systems*, pp. 16, 2021b.
- Kaiming He, Xiangyu Zhang, Shaoqing Ren, and Jian Sun. Deep Residual Learning for Image Recognition. In *2016 IEEE Conference on Computer Vision and Pattern Recognition (CVPR)*, pp. 770–778, Las Vegas, NV, USA, June 2016. IEEE. ISBN 978-1-4673-8851-1. doi: 10.1109/CVPR.2016.90. URL <http://ieeexplore.ieee.org/document/7780459/>.
- Dan Hendrycks and Thomas Dietterich. Benchmarking Neural Network Robustness to Common Corruptions and Perturbations. In *International Conference on Learning Representations*, 2019. URL <http://arxiv.org/abs/1903.12261>.

- Dan Hendrycks, Steven Basart, Norman Mu, Saurav Kadavath, Frank Wang, Evan Dorundo, Rahul Desai, Tyler Zhu, Samyak Parajuli, Mike Guo, Dawn Song, Jacob Steinhardt, and Justin Gilmer. The Many Faces of Robustness: A Critical Analysis of Out-of-Distribution Generalization. In *International Conference on Computer Vision*, pp. 10, 2021a.
- Dan Hendrycks, Kevin Zhao, Steven Basart, Jacob Steinhardt, and Dawn Song. Natural Adversarial Examples. In *Proceedings of the IEEE/CVF Conference on Computer Vision and Pattern Recognition*, pp. 15262–15271, 2021b. URL [https://openaccess.thecvf.com/content/CVPR2021/html/Hendrycks\\_Natural\\_Adversarial\\_Examples\\_CVPR\\_2021\\_paper.html](https://openaccess.thecvf.com/content/CVPR2021/html/Hendrycks_Natural_Adversarial_Examples_CVPR_2021_paper.html).
- Lei Hsiung, Yun-Yun Tsai, Pin-Yu Chen, and Tsung-Yi Ho. Towards Compositional Adversarial Robustness: Generalizing Adversarial Training to Composite Semantic Perturbations. In *IEEE Conference on Computer Vision and Pattern Recognition (CVPR)*, 2023.
- Jie Hu, Li Shen, and Gang Sun. Squeeze-and-Excitation Networks. In *Proceedings of the IEEE Conference on Computer Vision and Pattern Recognition*, pp. 7132–7141, 2018. URL [https://openaccess.thecvf.com/content\\_cvpr\\_2018/html/Hu\\_Squeeze-and-Excitation\\_Networks\\_CVPR\\_2018\\_paper.html](https://openaccess.thecvf.com/content_cvpr_2018/html/Hu_Squeeze-and-Excitation_Networks_CVPR_2018_paper.html).
- Gao Huang, Zhuang Liu, Laurens Van Der Maaten, and Kilian Q. Weinberger. Densely Connected Convolutional Networks. In *2017 IEEE Conference on Computer Vision and Pattern Recognition (CVPR)*, pp. 2261–2269, Honolulu, HI, July 2017. IEEE. ISBN 978-1-5386-0457-1. doi: 10.1109/CVPR.2017.243. URL <https://ieeexplore.ieee.org/document/8099726/>.
- Shihua Huang, Zhichao Lu, Kalyanmoy Deb, and Vishnu Naresh Boddeti. Revisiting Residual Networks for Adversarial Robustness. In *Proceedings of the IEEE/CVF Conference on Computer Vision and Pattern Recognition*, 2023.
- Max Kaufmann, Daniel Kang, Yi Sun, Steven Basart, Xuwang Yin, Mantas Mazeika, Akul Arora, Adam Dziedzic, Franziska Boenisch, Tom Brown, Jacob Steinhardt, and Dan Hendrycks. Testing Robustness Against Unforeseen Adversaries, July 2023. URL <http://arxiv.org/abs/1908.08016>. arXiv:1908.08016 [cs, stat].
- Klim Kireev, Maksym Andriushchenko, and Nicolas Flammarion. On the effectiveness of adversarial training against common corruptions. In *Proceedings of the Thirty-Eighth Conference on Uncertainty in Artificial Intelligence*, pp. 1012–1021. PMLR, August 2022. URL <https://proceedings.mlr.press/v180/kireev22a.html>. ISSN: 2640-3498.
- Cassidy Laidlaw and Soheil Feizi. Functional Adversarial Attacks. In *Advances in Neural Information Processing Systems*, volume 32. Curran Associates, Inc., 2019. URL <https://proceedings.neurips.cc/paper/2019/hash/6e923226e43cd6fac7cfe13ad000ac-Abstract.html>.
- Cassidy Laidlaw, Sahil Singla, and Soheil Feizi. Perceptual Adversarial Robustness: Defense Against Unseen Threat Models. In *International Conference on Learning Representations*, January 2021. URL <https://openreview.net/forum?id=dFwBosAcJkN>.
- Lin Li and Michael Spratling. Understanding and combating robust overfitting via input loss landscape analysis and regularization. *Pattern Recognition*, 136:109229, April 2023a. ISSN 0031-3203. doi: 10.1016/j.patcog.2022.109229. URL <https://www.sciencedirect.com/science/article/pii/S0031320322007087>.
- Lin Li and Michael W. Spratling. Data augmentation alone can improve adversarial training. In *The Eleventh International Conference on Learning Representations*, February 2023b. URL <https://openreview.net/forum?id=y4uc4NtTWaq>.
- Lin Li, Jianing Qiu, and Michael Spratling. AROID: Improving Adversarial Robustness through Online Instance-wise Data Augmentation, June 2023. URL <http://arxiv.org/abs/2306.07197>. arXiv:2306.07197 [cs].



- Chang Liu, Yinpeng Dong, Wenzhao Xiang, Xiao Yang, Hang Su, Jun Zhu, Yuefeng Chen, Yuan He, Hui Xue, and Shibao Zheng. A Comprehensive Study on Robustness of Image Classification Models: Benchmarking and Rethinking, February 2023. URL <http://arxiv.org/abs/2302.14301>. arXiv:2302.14301 [cs].
- Ze Liu, Yutong Lin, Yue Cao, Han Hu, Yixuan Wei, Zheng Zhang, Stephen Lin, and Baining Guo. Swin Transformer: Hierarchical Vision Transformer Using Shifted Windows. In *Proceedings of the IEEE/CVF International Conference on Computer Vision*, pp. 10012–10022, 2021. URL [https://openaccess.thecvf.com/content/ICCV2021/html/Liu\\_Swin\\_Transformer\\_Hierarchical\\_Vision\\_Transformer\\_Using\\_Shifted\\_Windows\\_ICCV\\_2021\\_paper.html](https://openaccess.thecvf.com/content/ICCV2021/html/Liu_Swin_Transformer_Hierarchical_Vision_Transformer_Using_Shifted_Windows_ICCV_2021_paper.html).
- Zhuang Liu, Hanzi Mao, Chao-Yuan Wu, Christoph Feichtenhofer, Trevor Darrell, and Saining Xie. A ConvNet for the 2020s. In *IEEE Conference on Computer Vision and Pattern Recognition (CVPR)*, 2022.
- Shangyun Lu, Bradley Nott, Aaron Olson, Alberto Todeschini, Hossein Vahabi, Yair Carmon, and Ludwig Schmidt. Harder or Different? A Closer Look at Distribution Shift in Dataset Reproduction. In *ICML 2020 Workshop on Uncertainty and Robustness in Deep Learning*, 2020.
- Aleksander Madry, Aleksandar Makelov, Ludwig Schmidt, Dimitris Tsipras, and Adrian Vladu. Towards Deep Learning Models Resistant to Adversarial Attacks. In *International Conference on Learning Representations*, 2018. URL <http://arxiv.org/abs/1706.06083>.
- Pratyush Maini, Eric Wong, and Zico Kolter. Adversarial Robustness Against the Union of Multiple Perturbation Models. In *Proceedings of the 37th International Conference on Machine Learning*, pp. 6640–6650. PMLR, November 2020. URL <https://proceedings.mlr.press/v119/maini20a.html>. ISSN: 2640-3498.
- Xiaofeng Mao, Yuefeng Chen, Xiaodan Li, Gege Qi, Ranjie Duan, Rong Zhang, and Hui Xue. Easyrobust: A comprehensive and easy-to-use toolkit for robust computer vision. <https://github.com/alibaba/easyrobust>, 2022.
- John P. Miller, Rohan Taori, Aditi Raghunathan, Shiori Sagawa, Pang Wei Koh, Vaishal Shankar, Percy Liang, Yair Carmon, and Ludwig Schmidt. Accuracy on the Line: on the Strong Correlation Between Out-of-Distribution and In-Distribution Generalization. In *Proceedings of the 38th International Conference on Machine Learning*, pp. 7721–7735. PMLR, July 2021. URL <https://proceedings.mlr.press/v139/miller21b.html>. ISSN: 2640-3498.
- Samuel G. Müller and Frank Hutter. TrivialAugment: Tuning-Free Yet State-of-the-Art Data Augmentation. In *Proceedings of the IEEE/CVF International Conference on Computer Vision*, pp. 774–782, 2021. URL [https://openaccess.thecvf.com/content/ICCV2021/html/Muller\\_TrivialAugment\\_Tuning-Free\\_Yet\\_State-of-the-Art\\_Data\\_Augmentation\\_ICCV\\_2021\\_paper.html](https://openaccess.thecvf.com/content/ICCV2021/html/Muller_TrivialAugment_Tuning-Free_Yet_State-of-the-Art_Data_Augmentation_ICCV_2021_paper.html).
- Tianyu Pang, Xiao Yang, Yinpeng Dong, Kun Xu, Jun Zhu, and Hang Su. Boosting Adversarial Training with Hypersphere Embedding. In *Advances in Neural Information Processing Systems*, volume 33, pp. 7779–7792. Curran Associates, Inc., 2020. URL <https://proceedings.neurips.cc/paper/2020/hash/5898d8095428ee310bf7fa3da1864ff7-Abstract.html>.
- Tianyu Pang, Min Lin, Xiao Yang, Jun Zhu, and Shuicheng Yan. Robustness and Accuracy Could Be Reconcilable by (Proper) Definition. In *Proceedings of the 39th International Conference on Machine Learning*, pp. 17258–17277. PMLR, June 2022. URL <https://proceedings.mlr.press/v162/pang22a.html>. ISSN: 2640-3498.
- Rahul Rade and Seyed-Mohsen Moosavi-Dezfooli. Reducing Excessive Margin to Achieve a Better Accuracy vs. Robustness Trade-off. In *International Conference on Learning Representations*, March 2022. URL <https://openreview.net/forum?id=Azh9QBQ4tR7>.
- Sylvestre-Alvise Rebuffi, Sven Gowal, Dan A. Calian, Florian Stimberg, Olivia Wiles, and Timothy Mann. Fixing Data Augmentation to Improve Adversarial Robustness. Technical Report arXiv:2103.01946, arXiv, October 2021. URL <http://arxiv.org/abs/2103.01946>. arXiv:2103.01946 [cs] type: article.

- Benjamin Recht, Rebecca Roelofs, Ludwig Schmidt, and Vaishal Shankar. Do CIFAR-10 Classifiers Generalize to CIFAR-10? *arXiv:1806.00451 [cs, stat]*, June 2018. URL <http://arxiv.org/abs/1806.00451>. arXiv: 1806.00451.
- Benjamin Recht, Rebecca Roelofs, Ludwig Schmidt, and Vaishal Shankar. Do ImageNet Classifiers Generalize to ImageNet? In *Proceedings of the 36th International Conference on Machine Learning*, pp. 12, 2019.
- Leslie Rice, Eric Wong, and J Zico Kolter. Overfitting in adversarially robust deep learning. In *Proceedings of the 37th International Conference on Machine Learning*, pp. 12, 2020.
- Jerome Rony, Luiz G. Hafemann, Luiz S. Oliveira, Ismail Ben Ayed, Robert Sabourin, and Eric Granger. Decoupling Direction and Norm for Efficient Gradient-Based L2 Adversarial Attacks and Defenses. In *2019 IEEE/CVF Conference on Computer Vision and Pattern Recognition (CVPR)*, pp. 4317–4325, Long Beach, CA, USA, June 2019. IEEE. ISBN 978-1-72813-293-8. doi: 10.1109/CVPR.2019.00445. URL <https://ieeexplore.ieee.org/document/8954314/>.
- Evgenia Rusak, Lukas Schott, Roland S. Zimmermann, Julian Bitterwolf, Oliver Bringmann, Matthias Bethge, and Wieland Brendel. A simple way to make neural networks robust against diverse image corruptions. In *Proceedings of the European Conference on Computer Vision*, 2020.
- M. Sandler, Andrew G. Howard, Menglong Zhu, A. Zhmoginov, and Liang-Chieh Chen. Mobilenetv2: Inverted residuals and linear bottlenecks. *IEEE/CVF Conference on Computer Vision and Pattern Recognition*, 2018. doi: 10.1109/CVPR.2018.00474.
- Vikash Sehwal, Arjun Nitin Bhagoji, Liwei Song, Chawin Sitawarin, Daniel Cullina, Mung Chiang, and Prateek Mittal. Analyzing the Robustness of Open-World Machine Learning. In *Proceedings of the 12th ACM Workshop on Artificial Intelligence and Security, AISec’19*, pp. 105–116, New York, NY, USA, November 2019. Association for Computing Machinery. ISBN 978-1-4503-6833-9. doi: 10.1145/3338501.3357372. URL <https://dl.acm.org/doi/10.1145/3338501.3357372>.
- Vikash Sehwal, Saeed Mahlouiifar, Tinashe Handina, Sihui Dai, Chong Xiang, Mung Chiang, and Prateek Mittal. Robust Learning Meets Generative Models: Can Proxy Distributions Improve Adversarial Robustness? In *International Conference on Learning Representations*, March 2022. URL <https://openreview.net/forum?id=WVX0NNVBBkV>.
- Karen Simonyan and Andrew Zisserman. Very Deep Convolutional Networks for Large-Scale Image Recognition. In *International Conference on Learning Representations*, 2015. URL <http://arxiv.org/abs/1409.1556>. arXiv: 1409.1556.
- Naman D. Singh, Francesco Croce, and Matthias Hein. Revisiting Adversarial Training for ImageNet: Architectures, Training and Generalization across Threat Models, March 2023. URL <http://arxiv.org/abs/2303.01870>. arXiv:2303.01870 [cs].
- David Stutz, Matthias Hein, and Bernt Schiele. Confidence-Calibrated Adversarial Training: Generalizing to Unseen Attacks. In *International Conference on Machine Learning*, pp. 12, 2020.
- Jiachen Sun, Akshay Mehra, Bhavya Kailkhura, Pin-Yu Chen, Dan Hendrycks, Jihun Hamm, and Z. Morley Mao. Certified adversarial defenses meet out-of-distribution corruptions: Benchmarking robustness and simple baselines. In *Proceedings of the European Conference on Computer Vision*, 2022a.
- Jiachen Sun, Akshay Mehra, Bhavya Kailkhura, Pin-Yu Chen, Dan Hendrycks, Jihun Hamm, and Z. Morley Mao. A Spectral View of Randomized Smoothing Under Common Corruptions: Benchmarking and Improving Certified Robustness. In Shai Avidan, Gabriel Brostow, Moustapha Cissé, Giovanni Maria Farinella, and Tal Hassner (eds.), *Computer Vision – ECCV 2022*, Lecture Notes in Computer Science, pp. 654–671, Cham, 2022b. Springer Nature Switzerland. ISBN 978-3-031-19772-7. doi: 10.1007/978-3-031-19772-7\_38.

- Christian Szegedy, Wei Liu, Yangqing Jia, Pierre Sermanet, Scott Reed, Dragomir Anguelov, Dumitru Erhan, Vincent Vanhoucke, and Andrew Rabinovich. Going deeper with convolutions. In *2015 IEEE Conference on Computer Vision and Pattern Recognition (CVPR)*, pp. 1–9, Boston, MA, USA, June 2015. IEEE. ISBN 978-1-4673-6964-0. doi: 10.1109/CVPR.2015.7298594. URL <http://ieeexplore.ieee.org/document/7298594/>.
- Christian Szegedy, Vincent Vanhoucke, Sergey Ioffe, Jon Shlens, and Zbigniew Wojna. Rethinking the Inception Architecture for Computer Vision. In *2016 IEEE Conference on Computer Vision and Pattern Recognition (CVPR)*, pp. 2818–2826, Las Vegas, NV, USA, June 2016. IEEE. ISBN 978-1-4673-8851-1. doi: 10.1109/CVPR.2016.308. URL <http://ieeexplore.ieee.org/document/7780677/>.
- Mingxing Tan and Quoc Le. EfficientNet: Rethinking Model Scaling for Convolutional Neural Networks. In *Proceedings of the 36th International Conference on Machine Learning*, pp. 6105–6114, May 2019. URL <http://proceedings.mlr.press/v97/tan19a.html>. ISSN: 1938-7228 Section: Machine Learning.
- Rohan Taori, Achal Dave, Vaishal Shankar, Nicholas Carlini, Benjamin Recht, and Ludwig Schmidt. Measuring Robustness to Natural Distribution Shifts in Image Classification. In *Advances in Neural Information Processing Systems*, volume 33, pp. 18583–18599. Curran Associates, Inc., 2020. URL <https://proceedings.neurips.cc/paper/2020/hash/d8330f857a17c53d217014ee776bfd50-Abstract.html>.
- Antonio Torralba, Rob Fergus, and William T. Freeman. 80 Million Tiny Images: A Large Data Set for Nonparametric Object and Scene Recognition. *IEEE Transactions on Pattern Analysis and Machine Intelligence*, 30(11):1958–1970, November 2008. ISSN 1939-3539. doi: 10.1109/TPAMI.2008.128. Conference Name: IEEE Transactions on Pattern Analysis and Machine Intelligence.
- Florian Tramer and Dan Boneh. Adversarial Training and Robustness for Multiple Perturbations. In *Advances in Neural Information Processing Systems*, volume 32. Curran Associates, Inc., 2019. URL <https://proceedings.neurips.cc/paper/2019/hash/5d4ae76f053f8f2516ad12961ef7fe97-Abstract.html>.
- Asher Trockman and J Zico Kolter. Patches are all you need? *Transactions on Machine Learning Research*, 2023. ISSN 2835-8856. URL <https://openreview.net/forum?id=rAnB7JSMXL>. Featured Certification.
- Yisen Wang, Difan Zou, Jinfeng Yi, James Bailey, Xingjun Ma, and Quanquan Gu. Improving Adversarial Robustness Requires Revisiting Misclassified Examples. In *International Conference on Learning Representations*, pp. 14, 2020.
- Zekai Wang, Tianyu Pang, Chao Du, Min Lin, Weiwei Liu, and Shuicheng Yan. Better Diffusion Models Further Improve Adversarial Training, February 2023. URL <http://arxiv.org/abs/2302.04638>. arXiv:2302.04638 [cs].
- Eric Wong, Leslie Rice, and J. Zico Kolter. Fast is better than free: Revisiting adversarial training. In *International Conference on Learning Representations*, 2020. URL <http://arxiv.org/abs/2001.03994>.
- Dongxian Wu, Shu-Tao Xia, and Yisen Wang. Adversarial Weight Perturbation Helps Robust Generalization. In *Advances in Neural Information Processing Systems*, volume 33, pp. 2958–2969, 2020. URL <https://papers.nips.cc/paper/2020/hash/1ef91c212e30e14bf125e9374262401f-Abstract.html>.
- Chaowei Xiao, Jun-Yan Zhu, Bo Li, Warren He, Mingyan Liu, and Dawn Song. Spatially Transformed Adversarial Examples. February 2018. URL <https://openreview.net/forum?id=HyydRMZC->.
- Saining Xie, Ross Girshick, Piotr Dollar, Zhuowen Tu, and Kaiming He. Aggregated Residual Transformations for Deep Neural Networks. pp. 1492–1500, 2017. URL [https://openaccess.thecvf.com/content\\_cvpr\\_2017/html/Xie\\_Aggregated\\_Residual\\_Transformations\\_CVPR\\_2017\\_paper.html](https://openaccess.thecvf.com/content_cvpr_2017/html/Xie_Aggregated_Residual_Transformations_CVPR_2017_paper.html).

- Yuancheng Xu, Yanchao Sun, Micah Goldblum, Tom Goldstein, and Furong Huang. Exploring and Exploiting Decision Boundary Dynamics for Adversarial Robustness. September 2022. URL <https://openreview.net/forum?id=aRTKuscKByJ>.
- Jingkang Yang, Pengyun Wang, Dejian Zou, Zitang Zhou, Kunyuan Ding, Wenxuan Peng, Haoqi Wang, Guangyao Chen, Bo Li, Yiyu Sun, Xuefeng Du, Kaiyang Zhou, Wayne Zhang, Dan Hendrycks, Yixuan Li, and Ziwei Liu. OpenOOD: Benchmarking generalized out-of-distribution detection, October 2022. URL <http://arxiv.org/abs/2210.07242>.
- Fisher Yu, Dequan Wang, Evan Shelhamer, and Trevor Darrell. Deep layer aggregation. In *2018 IEEE/CVF Conference on Computer Vision and Pattern Recognition*, pp. 2403–2412, 2018. doi: 10.1109/CVPR.2018.00255.
- Hongyang Zhang, Yaodong Yu, Jiantao Jiao, Eric Xing, Laurent El Ghaoui, and Michael Jordan. Theoretically Principled Trade-off between Robustness and Accuracy. In *International Conference on Machine Learning*, pp. 7472–7482. PMLR, May 2019. URL <http://proceedings.mlr.press/v97/zhang19p.html>. ISSN: 2640-3498.
- Jingfeng Zhang, Xilie Xu, Bo Han, Gang Niu, Lizhen Cui, Masashi Sugiyama, and Mohan Kankanhalli. Attacks Which Do Not Kill Training Make Adversarial Learning Stronger. In *Proceedings of the 37th International Conference on Machine Learning*, pp. 11278–11287. PMLR, November 2020. URL <https://proceedings.mlr.press/v119/zhang20z.html>. ISSN: 2640-3498.
- Richard Zhang, Phillip Isola, Alexei A. Efros, Eli Shechtman, and Oliver Wang. The Unreasonable Effectiveness of Deep Features as a Perceptual Metric. In *Proceedings of the IEEE Conference on Computer Vision and Pattern Recognition*, pp. 586–595, 2018. URL [https://openaccess.thecvf.com/content\\_cvpr\\_2018/html/Zhang\\_The\\_Unreasonable\\_Effectiveness\\_CVPR\\_2018\\_paper.html](https://openaccess.thecvf.com/content_cvpr_2018/html/Zhang_The_Unreasonable_Effectiveness_CVPR_2018_paper.html).
- Bingchen Zhao, Shaozuo Yu, Wufei Ma, Mingxin Yu, Shengxiao Mei, Angtian Wang, Ju He, Alan Yuille, and Adam Kortylewski. OOD-CV: A benchmark for robustness to out-of-distribution shifts of individual nuisances in natural images. In *Computer Vision – ECCV 2022: 17th European Conference, Tel Aviv, Israel, October 23–27, 2022, Proceedings, Part VIII*, pp. 163–180, Berlin, Heidelberg, 2022. Springer-Verlag. ISBN 978-3-031-20073-1. doi: 10.1007/978-3-031-20074-8\_10. URL [https://doi.org/10.1007/978-3-031-20074-8\\_10](https://doi.org/10.1007/978-3-031-20074-8_10).

## A BENCHMARK SET-UP

### A.1 DATASETS

This section introduces the OOD datasets of natural shifts. For ImageNet, we have:

- **ImageNet-V2** is a reproduction of ImageNet using a completely new set of images. It has the same 1000 classes as ImageNet and each class has 10 images so 10K images in total.
- **ImageNet-A** is an adversarially-selected reproduction of ImageNet. The images in this dataset were selected to be those most misclassified by an ensemble of ResNet-50s. It has 200 ImageNet classes and 7.5K images.
- **ImageNet-R** contains various artistic renditions of objects from ImageNet, so there is a domain shift. It has 30K images and 200 ImageNet classes.
- **ObjectNet** is a large real-world dataset for object recognition. It is constructed with controls to randomize background, object rotation and viewpoint. It has 313 classes but only 104 classes compatible with ImageNet classes so we only use this subset. The selected subset includes 17.2K images.

For CIFAR10, we have:

- **CIFAR10.1** is a reproduction of CIFAR10 using a completely new set of images. It has 2K images sampled from the same source as CIFAR10, i.e., 80M TinyImages (Torrallba et al., 2008). It has the same number of classes as CIFAR10.

- **CIFAR10.2** is another reproduction of CIFAR10. It has 12K (10k for training and 2k for test) images sampled from the same source as CIFAR10, i.e., 80M TinyImages. It has the same number of classes as CIFAR10. We only use the test set of CIFAR10.2.
- **CINIC** is a downsampled subset of ImageNet with the same image resolution and classes as CIFAR10. Its test set has 90K images in total, of which 20K images are from CIFAR10 and 70K images are from ImageNet. We use only the ImageNet part.
- **CIFAR10-R** is a new dataset created by us. The images in CIFAR10-R and CIFAR10 have different styles so there is a domain shift. We follow the same procedure as CINIC to downscale the images from ImageNet-R to the same resolution as CIFAR10 and select images from the classes of ImageNet corresponding to CIFAR10 classes. We follow the same class mapping between ImageNet and CIFAR10 as CINIC. Note that ImageNet-R does not have images of the ImageNet classes corresponding to CIFAR10 classes of "airplane" and "horse", so there are only 8 classes in CIFAR10-R.

In practice, we evaluate models using a random sample of 5K images from each of the ImageNet variant datasets, and 10K images from each of the CIFAR10 variant datasets, if those datasets contain more images than that number. This is done to accelerate the evaluation and follows the practice used in RobustBench (Croce et al., 2021).

## A.2 ADVERSARIAL EVALUATION

### A.2.1 SEEN ATTACKS

Robustness under dataset shift is evaluated using the same threat model as used in adversarial training, the so-called seen threat model. The perturbation bound  $\epsilon$  is  $8/255$  for CIFAR10  $\ell_\infty$ ,  $0.5$  for CIFAR10  $\ell_2$  and  $4/255$  for ImageNet  $\ell_\infty$ . We use the MM5 (Gao et al., 2022) attack, instead of other more effective attacks like AutoAttack (Croce & Hein, 2020), for a better balance of efficiency and effectiveness. MM5 is about  $32\times$  faster than AutoAttack (Gao et al., 2022). This makes OODRobustBench practical to use and also makes our large-scale analysis on hundreds of models feasible.

To verify the effectiveness of MM5, we compare its result with the result of AutoAttack on the ID dataset across all publicly available models from RobustBench for CIFAR10  $\ell_\infty$ , CIFAR10  $\ell_2$  and ImageNet  $\ell_\infty$ . The gap between the robustness evaluated by them is generally below  $0.5\%$ , except for two models: Ding et al. (2020) and Xu et al. (2022). We use MM+ (Gao et al., 2022) attack to evaluate these two models for a more reliable evaluation and the result of MM+ is close to AutoAttack.

### A.2.2 UNFORESEEN ATTACKS

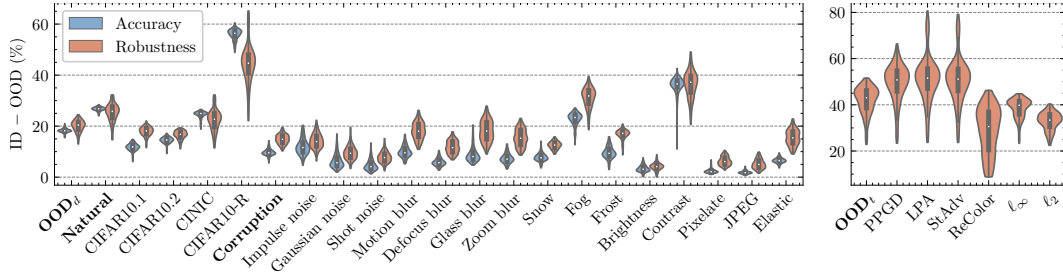
For non- $\ell_p$  shifts, we follow the same configuration of attacks as Laidlaw et al. (2021). Specifically, the perturbation bound is  $0.5$  for PPGD,  $0.5$  for LPA,  $0.05$  for StAdv and  $0.06$  for ReColor. The number of iterations is  $40$  for PPGD and LPA regardless of dataset, is  $100$  for StAdv and ReColor on CIFAR10 and  $200$  on ImageNet.

For  $\ell_p$  shifts all attacks are performed using MM5. The unforeseen attacks use  $\epsilon = 12/255$  and  $\epsilon = 0.5$  for  $\ell_\infty$  and  $\ell_2$  attacks on CIFAR10  $\ell_\infty$ ,  $\epsilon = 8/255$  and  $\epsilon = 1$  for  $\ell_\infty$  and  $\ell_2$  attacks on CIFAR10  $\ell_2$  and on ImageNet  $\ell_\infty$ .

## B MODEL ZOO

Our model zoo consists of 706 models, of which:

- 396 models are trained on CIFAR10 by  $\ell_\infty$   $8/255$
- 239 models are trained on CIFAR10 by  $\ell_2$   $0.5$
- 56 models are trained on ImageNet by  $\ell_\infty$   $4/255$
- 10 models are trained on CIFAR10 for non- $\ell_p$  adversarial robustness
- 5 models are trained on CIFAR10 for common corruption robustness

Figure 7: Degradation of accuracy and robustness under various distribution shifts for CIFAR10  $\ell_2$ .

Among the above models, 66 models of CIFAR10  $\ell_\infty$ , 19 models of CIFAR10  $\ell_2$  and 18 models of ImageNet  $\ell_\infty$  are retrieved from RobustBench. 84 models are retrieved from the published works including Li & Spratling (2023b); Li et al. (2023); Li & Spratling (2023a); Liu et al. (2023); Singh et al. (2023); Dai et al. (2022); Hsiung et al. (2023); Mao et al. (2022). The remaining models are trained by ourselves.

We locally train additional models with varying architectures and training parameters to complement the public models from RobustBench on CIFAR-10. We consider 20 model architectures: DenseNet-121 (Huang et al., 2017), GoogLeNet (Szegedy et al., 2015), Inception-V3 (Szegedy et al., 2016), VGG-11/13/16/19 (Simonyan & Zisserman, 2015), ResNet-34/50/101/152 (He et al., 2016), EfficientNet-B0 (Tan & Le, 2019), MobileNet-V2 (Sandler et al., 2018), DLA (Yu et al., 2018), ResNeXt-29 (2x64d/4x64d/32x4d/8x64d) (Xie et al., 2017), SeNet-18 (Hu et al., 2018), and ConvMixer (Trockman & Kolter, 2023). For each architecture, we vary the training procedure to obtain 15 models across four adversarial training methods: PGD (Madry et al., 2018), TRADES (Zhang et al., 2019), PGD-SCORE, and TRADES-SCORE (Pang et al., 2022).

We train all models under both  $\ell_\infty$  and  $\ell_2$  threat models with the following steps:

1. We use PGD adversarial training to train eight models with batch size  $\in \{128, 512\}$ , a learning rate  $\in \{0.1, 0.05\}$ , and weight decay  $\in \{10^{-4}, 10^{-5}\}$ . We also save the overall best hyperparameter choice. For the  $\ell_2$  threat model, we fix the learning rate to 0.1 since we observe that with  $\ell_\infty$ , 0.1 is strictly better than 0.05.
2. Using the best hyperparameter choice, we train one model with PGD-SCORE, three with TRADES, and three with TRADES-SCORE. For TRADES and TRADES-SCORE, we take their  $\beta$  parameter from 0.1, 0.3, 1.0.

After training, we observe that some locally trained models exhibit inferior accuracy and/or robustness that is abnormally lower than others. The influence of inferior models on the correlation analysis is discussed in App. E. Finally, we filter out all models with an overall performance (accuracy + robustness) below 110. This threshold is determined to exclude only those evidently inferior models so that the size of model zoo (557 after filtering) is still large enough to ensure the generality and comprehensiveness of the conclusions drawn on it.

## C ADDITIONAL RESULT

### C.1 BENCHMARK

- Tab. 2: benchmark result of state-of-the-art methods for CIFAR10  $\ell_2$ .
- Tab. 3: benchmark result of state-of-the-art methods for ImageNet  $\ell_\infty$ .

### C.2 PERFORMANCE DEGRADATION DISTRIBUTION

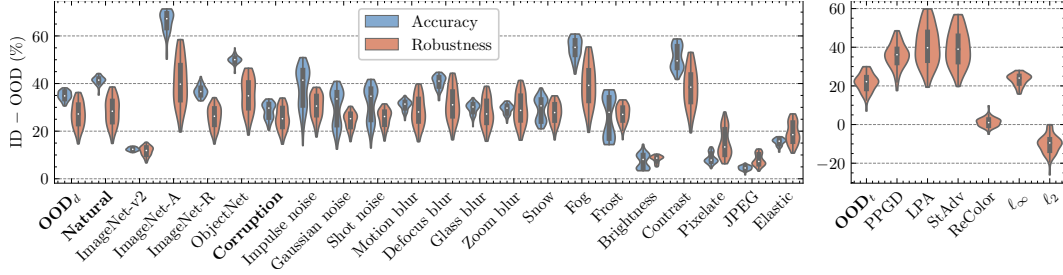
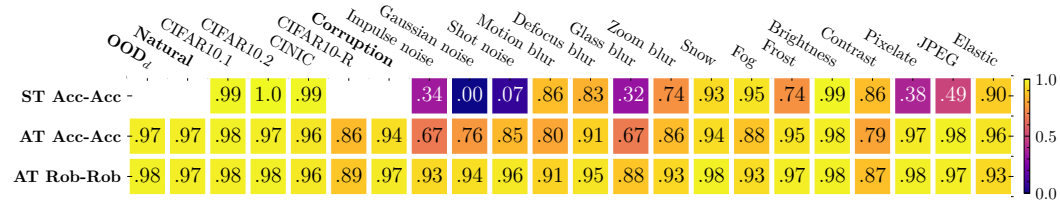
- Fig. 7: performance degradation distribution for CIFAR10  $\ell_2$
- Fig. 8: performance degradation distribution for ImageNet  $\ell_\infty$ .

Table 2: Performance, evaluated with OODRobustBench, of state-of-the-art models trained on CIFAR10 to be robust to  $\ell_2$  attacks. Top 3 results under each metric are highlighted by **bold** and/or underscore. The column “OOD” gives the overall OOD robustness which is the mean of the robustness to  $\text{OOD}_d$  and  $\text{OOD}_t$ .

Method	Accuracy		Robustness				Ranking (Rob.)	
	ID	$\text{OOD}_d$	ID	$\text{OOD}_d$	$\text{OOD}_t$	OOD	ID	OOD
Wang et al. (2023) (WRN-70-16)	<b>95.54</b>	<b>80.04</b>	<b>84.97</b>	<b>60.83</b>	<b>36.65</b>	<b>48.74</b>	1	1
Wang et al. (2023) (WRN-28-10)	95.16	79.28	<b>83.69</b>	<b>59.39</b>	<b>35.04</b>	<b>47.21</b>	2	2
Rebuffi et al. (2021) (WRN-70-16-cutmix-extra)	<b>95.74</b>	<b>79.90</b>	82.36	57.94	31.71	44.82	3	4
Gowal et al. (2021a) (extra)	94.74	78.78	80.56	56.18	30.48	43.33	4	6
Rebuffi et al. (2021) (WRN-70-16-cutmix-ddpm)	92.41	75.95	80.42	56.82	34.58	45.70	5	3
Augustin et al. (2020) (WRN-34-10-extra)	93.97	77.40	78.81	54.71	31.62	43.16	6	7
Rebuffi et al. (2021) (WRN-28-10-cutmix-ddpm)	91.79	75.26	78.79	55.63	33.32	44.48	7	5
Sehwag et al. (2022)	90.93	74.00	77.29	54.33	29.44	41.88	8	8
Augustin et al. (2020) (WRN-34-10)	92.23	76.43	76.27	52.83	29.25	41.04	9	11
Rade & Moosavi-Dezfooli (2022)	90.57	73.55	76.14	53.35	29.69	41.52	10	9
Rebuffi et al. (2021) (R18-cutmix-ddpm)	90.33	72.96	75.87	52.21	30.06	41.14	11	10
Gowal et al. (2021a)	90.89	74.71	74.51	52.20	25.76	38.98	12	15
Sehwag et al. (2022) (R18)	89.76	72.31	74.42	51.76	26.68	39.22	13	13
Wu et al. (2020)	88.51	71.23	73.66	51.53	27.50	39.52	14	12
Augustin et al. (2020)	91.07	74.24	72.99	49.32	28.72	39.02	15	14
Engstrom et al. (2019)	90.83	73.85	69.25	46.65	17.71	32.18	16	16
Rice et al. (2020)	88.67	71.27	67.69	44.76	18.58	31.67	17	17
Rony et al. (2019)	89.04	71.77	66.46	44.54	18.31	31.42	18	18
Ding et al. (2020)	88.00	72.32	66.09	43.79	16.52	30.15	19	20

Table 3: Performance, evaluated with OODRobustBench, of state-of-the-art models trained on ImageNet to be robust to  $\ell_\infty$  attacks. Top 3 results under each metric are highlighted by **bold** and/or underscore. The column “OOD” gives the overall OOD robustness which is the mean of the robustness to  $\text{OOD}_d$  and  $\text{OOD}_t$ .

Method	Accuracy		Robustness				Ranking (Rob.)	
	ID	$\text{OOD}_d$	ID	$\text{OOD}_d$	$\text{OOD}_t$	OOD	ID	OOD
Liu et al. (2023) (Swin-L)	<b>78.92</b>	<b>45.84</b>	<b>59.82</b>	<b>23.59</b>	<b>29.88</b>	<b>26.74</b>	1	1
Liu et al. (2023) (ConvNeXt-L)	<b>78.02</b>	<b>44.74</b>	<b>58.76</b>	<b>23.35</b>	<b>30.10</b>	<b>26.72</b>	2	2
Singh et al. (2023) (ConvNeXt-L-ConvStem)	77.00	44.05	57.82	23.09	27.98	25.53	3	3
Liu et al. (2023) (Swin-B)	76.16	42.58	56.26	21.45	27.02	24.24	4	7
Singh et al. (2023) (ConvNeXt-B-ConvStem)	75.88	42.29	56.24	21.77	27.89	24.83	5	5
Liu et al. (2023) (ConvNeXt-B)	76.70	43.06	56.02	21.74	26.97	24.36	6	6
Singh et al. (2023) (ViT-B-ConvStem)	76.30	44.67	54.90	21.76	28.98	25.37	7	4
Singh et al. (2023) (ConvNeXt-S-ConvStem)	74.08	39.55	52.66	19.35	26.87	23.11	8	9
Singh et al. (2023) (ConvNeXt-B)	75.08	40.68	52.44	20.09	26.06	23.07	9	10
Liu et al. (2023) (Swin-S)	75.20	40.84	52.10	19.67	24.73	22.20	10	12
Liu et al. (2023) (ConvNeXt-S)	75.64	40.91	51.66	19.40	25.00	22.20	11	11
Singh et al. (2023) (ConvNeXt-T-ConvStem)	72.70	38.15	49.46	17.97	25.32	21.65	12	14
Singh et al. (2023) (ViT-S-ConvStem)	72.58	39.24	48.46	17.83	25.43	21.63	13	15
Singh et al. (2023) (ViT-B)	72.98	42.38	48.34	20.43	26.26	23.34	14	8
Debenedetti et al. (2023) (XCiT-L12)	73.78	38.10	47.88	15.84	23.22	19.53	15	18
Singh et al. (2023) (ViT-M)	71.78	39.88	47.34	18.95	25.25	22.10	16	13
Singh et al. (2023) (ConvNeXt-T)	71.88	37.70	46.98	17.13	21.36	19.25	17	19
Mao et al. (2022) (Swin-B)	74.14	38.45	46.54	15.36	22.19	18.78	18	20
Liu et al. (2023) (ViT-B)	72.84	39.88	45.90	18.01	22.95	20.48	19	16
Debenedetti et al. (2023) (XCiT-M12)	74.04	37.00	45.76	14.73	22.82	18.77	20	21

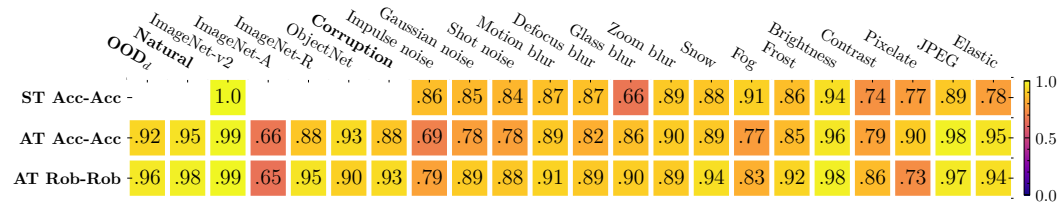
Figure 8: Degradation of accuracy and robustness under various distribution shifts for ImageNet  $\ell_\infty$ .Figure 9:  $R^2$  of regression between ID and OOD performance for Standardly-Trained (ST) and Adversarially-Trained (AT) models under various dataset shifts for CIFAR10  $\ell_2$ . Higher  $R^2$  implies stronger linear correlation. The result of ST models is copied from Miller et al. (2021).

### C.3 CORRELATION BETWEEN ID AND OOD PERFORMANCE UNDER DATASET SHIFTS

- Fig. 9:  $R^2$  of regressions for Acc-Acc and Rob-Rob for CIFAR10  $\ell_2$ .
- Fig. 10:  $R^2$  of regressions for Acc-Acc and Rob-Rob for ImageNet  $\ell_\infty$ .
- Fig. 11:  $R^2$  of regressions for Acc-Rob and Rob-Acc for CIFAR10  $\ell_\infty$ , CIFAR10  $\ell_2$  and ImageNet  $\ell_\infty$ .

### C.4 PREDICTED UPPER LIMIT OF OOD ACCURACY AND ROBUSTNESS

- Fig. 12: the estimated upper limit of OOD accuracy and the conversion rate for CIFAR10  $\ell_\infty$ .
- Fig. 13: the estimated upper limit of OOD performance and the conversion rate for CIFAR10  $\ell_2$ .
- Fig. 14: the estimated upper limit of OOD performance and the conversion rate for ImageNet  $\ell_\infty$ .

Figure 10:  $R^2$  of regression between ID and OOD performance for Standardly-Trained (ST) and Adversarially-Trained (AT) models under various dataset shifts for ImageNet  $\ell_\infty$ . Higher  $R^2$  implies stronger linear correlation. The result of ST models is copied from Miller et al. (2021).



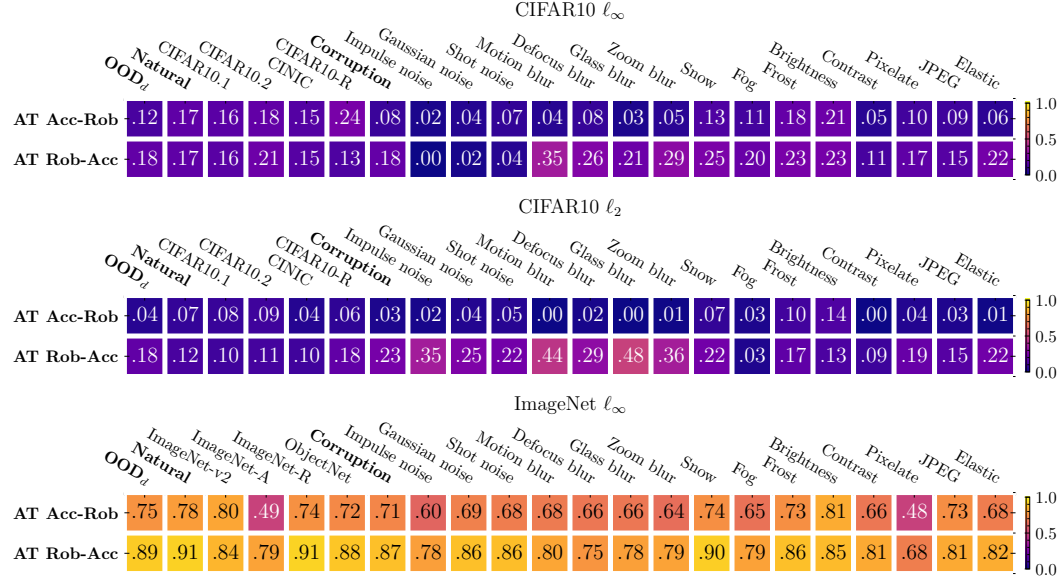


Figure 11:  $R^2$  of regression between ID and OOD performance for Adversarially-Trained (AT) models under various dataset shifts. "Acc-Rob" denotes the linear model between ID accuracy (x) and OOD robustness (y) and "Rob-Acc" for ID robustness (x) and OOD accuracy (y).

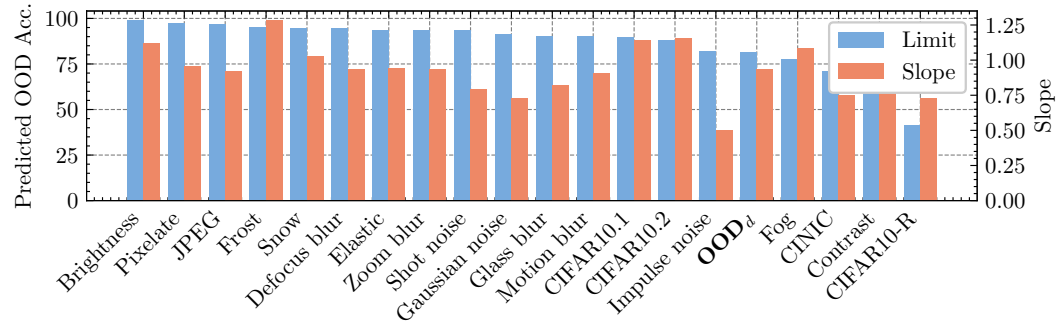


Figure 12: The estimated upper limit of OOD accuracy and the conversion rate, a.k.a. slope, to OOD accuracy from ID accuracy under various distribution shifts for CIFAR10  $\ell_\infty$ .

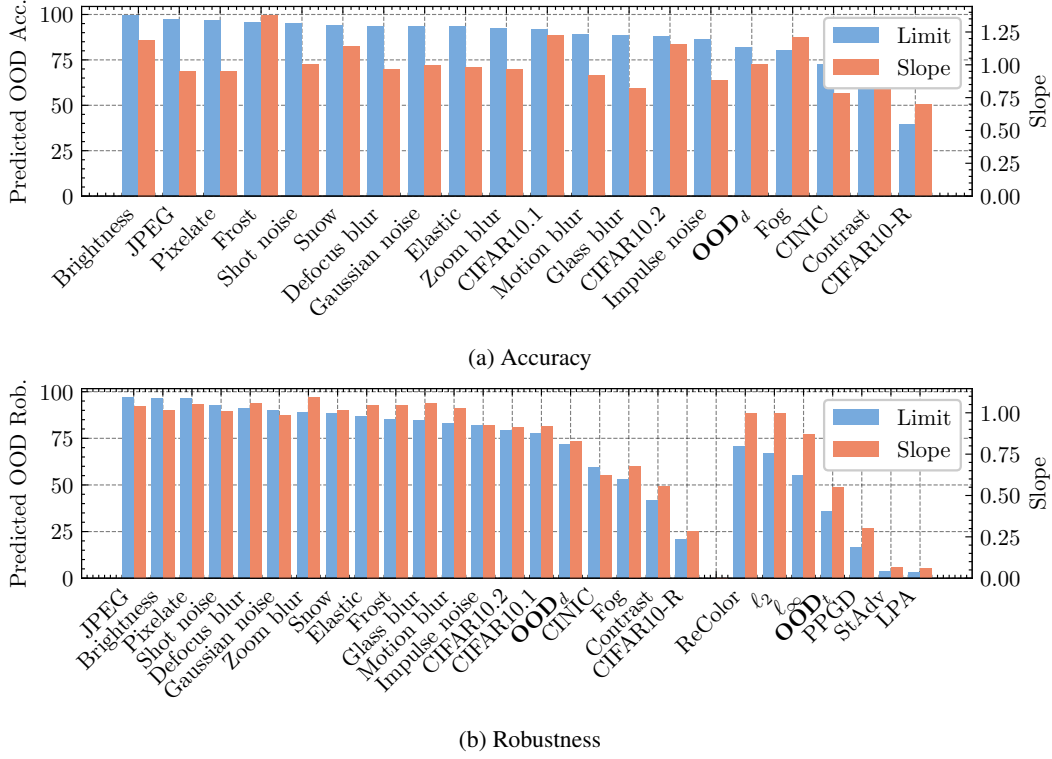


Figure 13: The estimated upper limit of OOD performance and the conversion rate, a.k.a. slope, to OOD performance from ID performance under various distribution shifts for CIFAR10  $\ell_2$ .

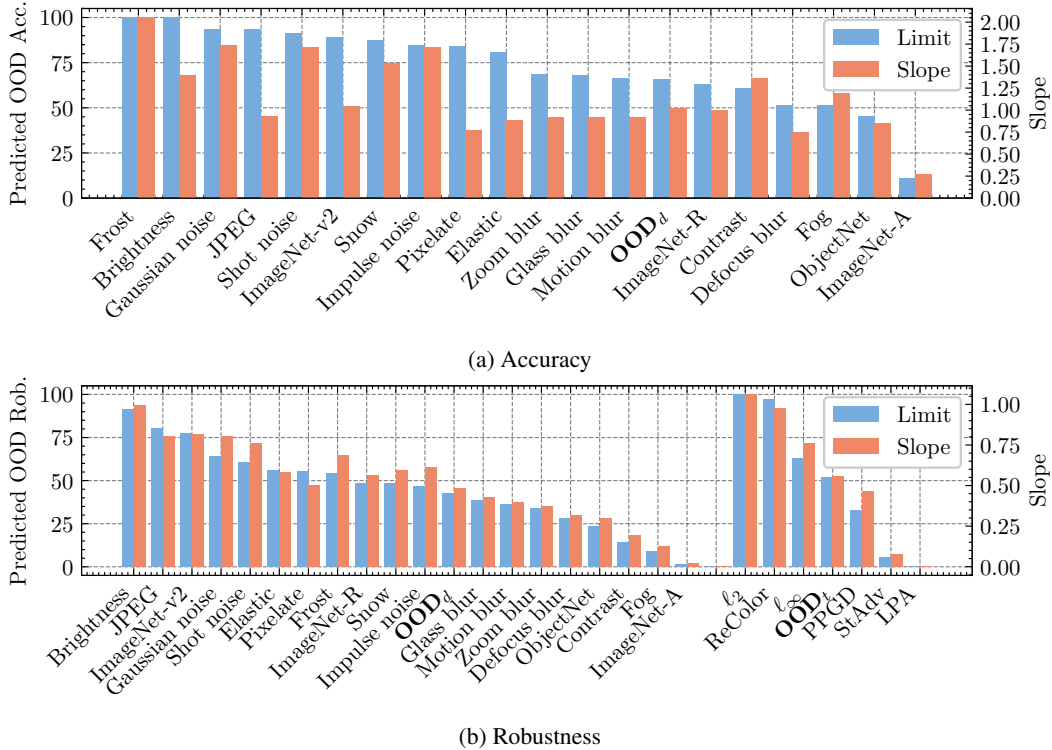


Figure 14: The estimated upper limit of OOD performance and the conversion rate, a.k.a. slope, to OOD performance from ID performance under various distribution shifts for ImageNet  $\ell_\infty$ .

## D CATASTROPHIC DEGRADATION OF ROBUSTNESS

We observe this issue on only one implementation, using WideResNet28-10 with extra synthetic data (model id: *Rade2021Helper\_ddpm* on RobustBench), from Rade & Moosavi-Dezfooli (2022) for CIFAR10  $\ell_\infty$ . There are three other implementations of this method on RobustBench. None of them, including the one using ResNet18 with extra synthetic data, is observed to suffer from this issue. It seems that catastrophic degradation in this case is specific to the implementation or training dynamics.

On the other hand, catastrophic degradation consistently happens on the models trained with AutoAugment or IDBH but not other tested data augmentations. It suggests the possibility that a certain image transformation operation exclusively used by AutoAugment and IDBH cause this issue. Besides, catastrophic degradation also consistently happens on the models trained using the receipt of Debenedetti et al. (2023) under Gaussian and shot noise shifts. However, it employs a wide range of training techniques, so further experiments are required to identify the specific cause.

## E HOW INFERIOR MODELS AFFECT THE CORRELATION ANALYSIS

This section studies the influence of the construction of model zoo on the result of correlation. We use the overall performance (accuracy + robustness) to filter out inferior models. As we increasing the threshold of overall performance for filtering, the average overall performance of the model zoo increases, the number of included models decreases and the weight of the models from other published sources on the regression grows up. Our locally trained models are normally inferior to the public models regarding the performance since the latter employs better optimized and more effective training methods and settings. The training methods and settings of public models are also much more diverse.

The correlation for particular shifts varies considerably as more inferior models removed.  $R^2$  declines considerably under CIFAR10-R, noise, fog, glass blur, frost and contrast for both Acc-Acc and Rob-Rob on CIFAR10  $\ell_\infty$  (Fig. 15) and  $\ell_2$  (Fig. 16). A similar trend is also observed for threat shifts, ReColor and different  $p$ -norm for CIFAR10  $\ell_\infty$  as shown in Fig. 17. It suggests that the weak correlation under these shifts mainly results from those high-performance public models, and is likely related to the fact that these models include much diverse training methods and settings. For example, all observed catastrophic degradation under the noise shifts occur in the public models. Note that the locally trained models have a large diversity in model architectures particularly within the family of CNNs, but it seems that this architectural diversity does not effect the correlation as much as other factors.

In contrast, correlation is improved for most threat shifts for CIFAR10  $\ell_2$  as shown in Fig. 17. As shown in Fig. 25, the locally trained (inferior) models and the public (high-performance) models have divergent linear trends (most evident in the plot of PPGD). That’s why removing models from either group will enhance the correlation. Note that such divergence is not evident in the figures of CIFAR10  $\ell_\infty$  (Fig. 24) and ImageNet  $\ell_\infty$  (Fig. 26).

## F EFFECTIVE ROBUST INTERVENTION

All models used in this analysis are retrieved from RobustBench or other published works to ensure they are well-trained by the techniques to be examined. For each robust intervention, some general training setting, the reference to the source of models and the detailed performance are summarized in the following tables:

- Tab. 4: training with extra data.
- Tab. 5: training with advanced data augmentation.
- Tab. 6: training with advanced model architectures.
- Tab. 7: scaling models up.
- Tab. 8: training techniques of VR, HE, MMA and AS.

The specific experiment setting for each model can be found in its original paper.

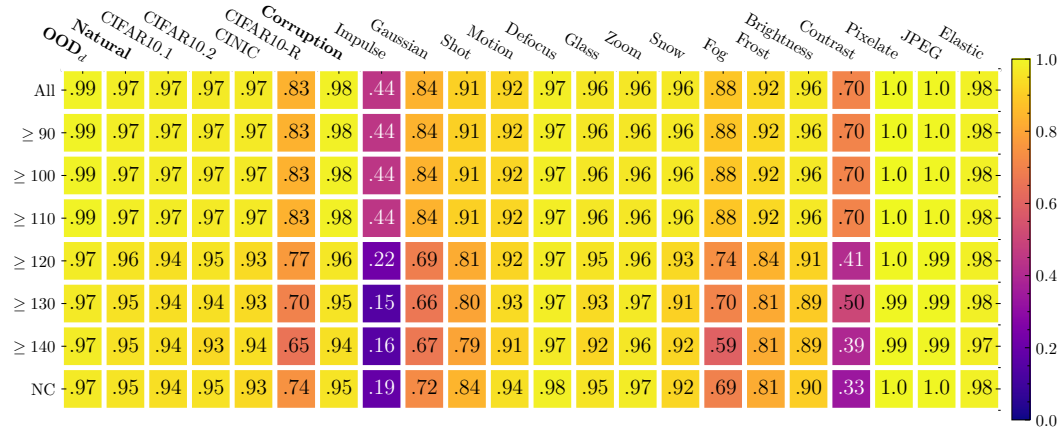
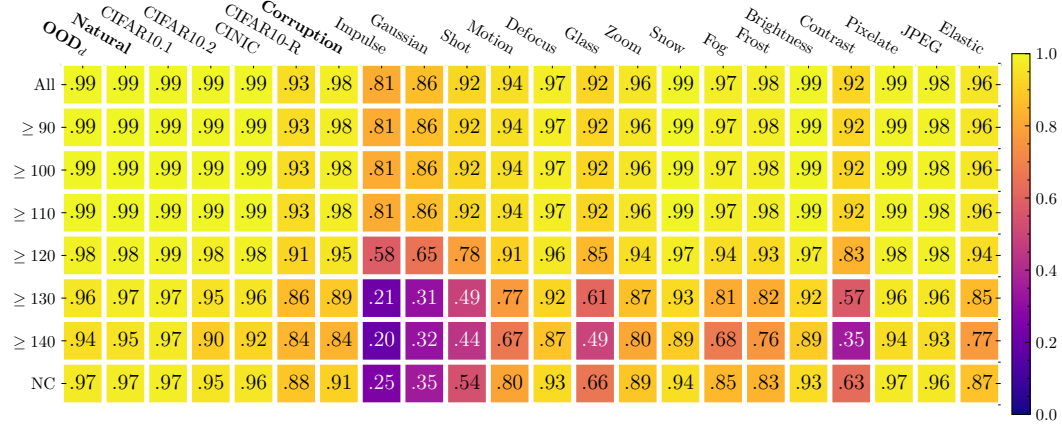
(a)  $R^2$  of Acc-Acc(b)  $R^2$  of Rob-Rob

Figure 15: How  $R^2$  under various dataset shifts changes as the models with lower overall performance are removed from regression for CIFAR10  $\ell_\infty$ . Each row, with the filtering threshold labeled at the lead, corresponds to a new filtered model zoo and the regression conducted on it. "NC" refers to No Custom models, so all models are retrieved from either RobustBench or other published works.

Table 4: The effect of training with extra data on the OOD generalization of accuracy and robustness.

Dataset	Threat Model	Training	Model Architecture	Extra Data	ID		OOD <sub>d</sub>				OOD <sub>t</sub>	
					Acc.	Rob.	Acc.	Rob.	EAcc.	ERob.	Rob.	ERob.
CIFAR10	Linf	Gowal et al. (2021a)	WideResNet70-16	-	85.29	57.24	66.98	35.90	-0.56	0.30	29.39	-2.18
				Synthetic	88.74	<b>66.24</b>	70.68	<b>42.76</b>	-0.08	<b>0.74</b>	33.65	-2.13
				Real	<b>91.10</b>	66.03	<b>73.24</b>	42.58	<b>0.26</b>	0.71	<b>34.00</b>	<b>-1.67</b>

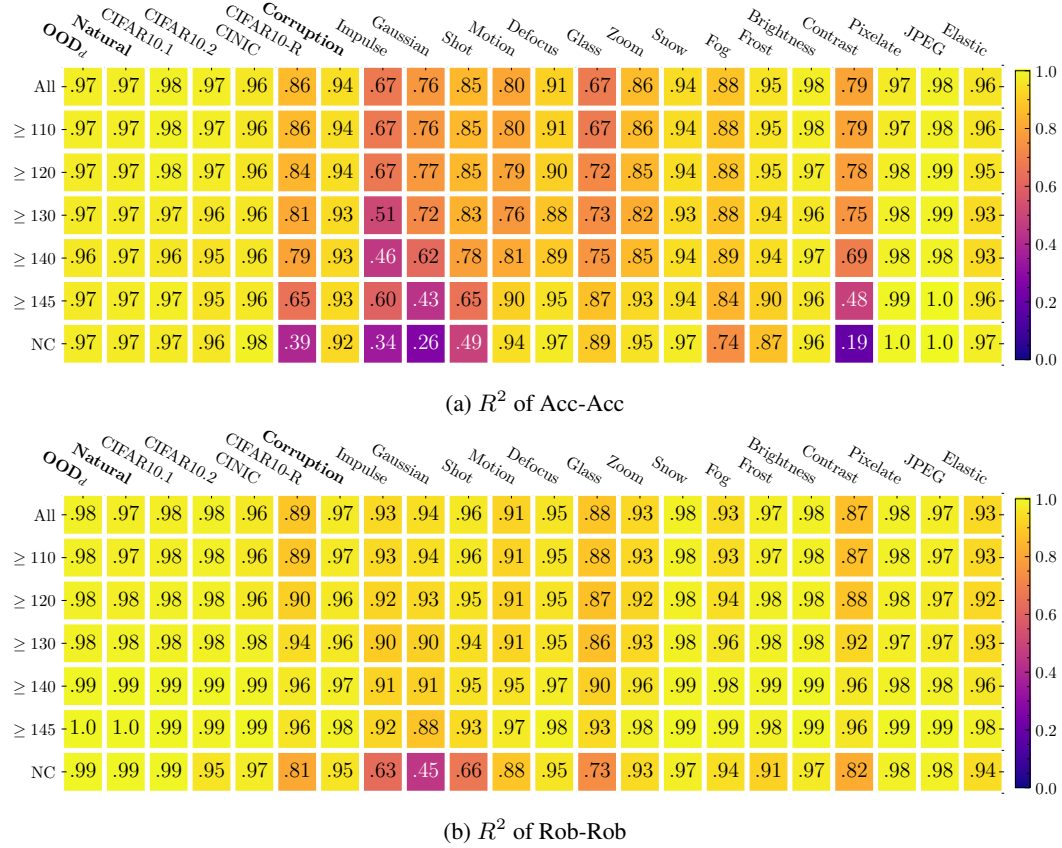


Figure 16: How  $R^2$  under various dataset shifts changes as the models with lower overall performance are removed from regression for CIFAR10  $\ell_2$ . Each row, with the filtering threshold labeled at the lead, corresponds to a new filtered model zoo and the regression conducted it. "NC" refers to No Custom models, so all models are retrieved from either RobustBench or other published works.

Table 5: The effect of data augmentation on the OOD generalization of accuracy and robustness. The results reported in Fig. 6b are the mean of the results on ViT and WideResNets.

Dataset	Threat Model	Training	Model Architecture	Data Augmentation	ID		OOD <sub>d</sub>				OOD <sub>t</sub>	
					Acc.	Rob.	Acc.	Rob.	EAcc.	ERob.	Rob.	ERob.
CIFAR10	Linf	Li & Spratling (2023b)	ViT-B	RandomCrop	83.23	47.02	66.48	28.85	0.86	0.54	27.36	0.57
				Cutout	<b>84.22</b>	<b>49.57</b>	<b>67.23</b>	<b>30.68</b>	0.69	0.56	29.74	1.75
				CutMix	80.92	47.45	63.93	29.89	0.48	<b>1.27</b>	30.48	3.49
				TrivialAugment	80.33	46.61	64.59	29.56	<b>1.69</b>	<b>1.54</b>	30.40	<b>3.80</b>
				AutoAugment	82.75	48.11	65.89	29.78	0.73	0.69	<b>30.90</b>	<b>3.60</b>
				IDBH	<b>86.92</b>	<b>51.55</b>	<b>70.51</b>	<b>32.08</b>	<b>1.45</b>	0.54	<b>30.59</b>	1.68
			WideResNet34-10	RandomCrop	86.52	52.42	68.11	31.55	-0.58	<b>-0.61</b>	26.47	-2.84
				Cutout	86.77	53.31	68.40	31.03	-0.53	-1.76	27.00	-2.74
				CutMix	87.41	53.89	68.97	31.71	-0.55	-1.50	28.50	<b>-1.50</b>
				TrivialAugment	86.98	54.18	69.85	<b>32.94</b>	<b>0.73</b>	<b>-0.47</b>	<b>28.62</b>	<b>-1.52</b>
				AutoAugment	<b>87.93</b>	<b>55.10</b>	<b>70.05</b>	32.17	0.04	-1.90	<b>29.06</b>	<b>-1.51</b>
				IDBH	<b>88.62</b>	<b>55.56</b>	<b>70.96</b>	<b>32.99</b>	<b>0.30</b>	-1.41	28.58	-2.21

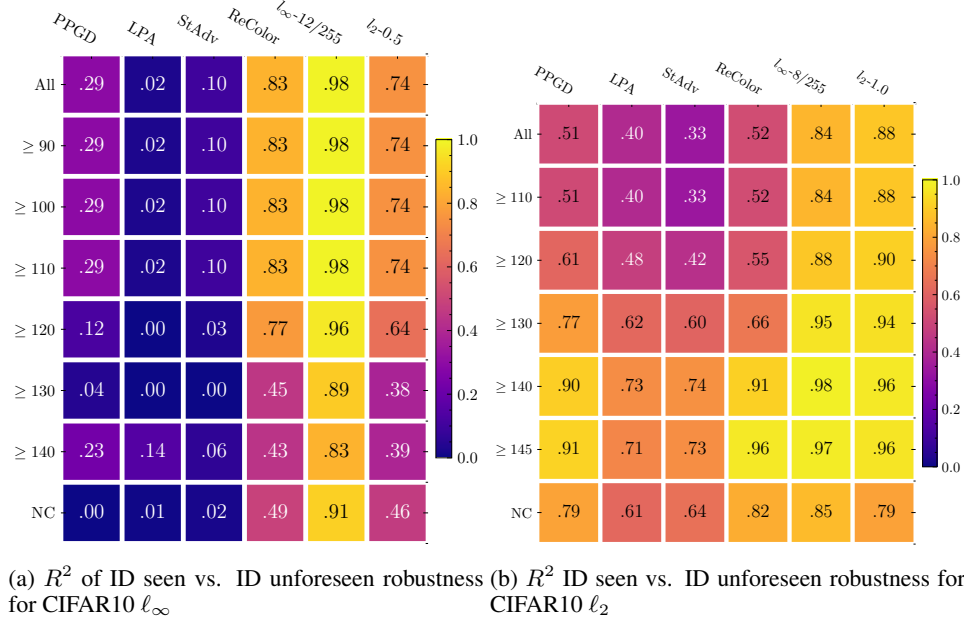


Figure 17: How  $R^2$  under various threat shifts changes as the models with lower overall performance are removed from regression. Each row, with the filtering threshold labeled at the lead, corresponds to a new filtered model zoo and the regression conducted it. "NC" refers to No Custom models, so all models are retrieved from either RobustBench or other published works.

Table 6: The effect of model architecture on the OOD generalization of accuracy and robustness.

Dataset	Threat Model	Training	Model Architecture	Model Size (M)	ID		OOD <sub>d</sub>				OOD <sub>t</sub>	
					Acc.	Rob.	Acc.	Rob.	EAcc.	ERob.	Rob.	ERob.
ImageNet	$\ell_\infty$	Liu et al. (2023)	ResNet152	60.19	70.92	43.62	34.43	14.13	-1.71	-1.26	17.23	-3.47
			ConvNeXt-B	<b>88.59</b>	<b>76.70</b>	56.02	<b>43.06</b>	<b>21.74</b>	1.03	0.33	26.97	-0.63
			ViT-B	86.57	72.84	45.90	39.88	18.01	<b>1.78</b>	<b>1.51</b>	22.95	<b>0.98</b>
			Swin-B	87.77	76.16	<b>56.26</b>	42.58	21.45	1.10	-0.07	<b>27.02</b>	-0.72

Table 7: The effect of model size on the OOD generalization of accuracy and robustness. The results reported in Fig. 6d are averaged over three architectures at the corresponding relatively model size. For example, the result of "small" is averaged over WideResNet28-10, ResNet50 and ConvNeXt-S-ConvStem.

Dataset	Threat Model	Training	Model Architecture	Model Size	ID		OOD <sub>d</sub>				OOD <sub>t</sub>	
					Acc.	Rob.	Acc.	Rob.	EAcc.	ERob.	Rob.	ERob.
CIFAR10	$\ell_\infty$	Rebuffi et al. (2021)	WideResNet28-10	36.48	87.33	60.88	69.35	38.54	-0.10	0.35	33.63	<b>0.36</b>
			WideResNet70-16	266.80	88.54	64.33	70.62	41.01	0.04	0.35	<b>34.12</b>	-0.76
			WideResNet106-16	<b>415.48</b>	<b>88.50</b>	<b>64.82</b>	<b>70.65</b>	<b>41.43</b>	<b>0.11</b>	<b>0.42</b>	33.90	-1.22
ImageNet	$\ell_\infty$	Liu et al. (2023)	ResNet50	25.56	65.02	32.02	28.43	9.23	<b>-1.68</b>	<b>-0.53</b>	13.71	<b>-0.52</b>
			ResNet101	44.55	68.34	39.76	31.74	12.44	-1.76	-1.08	16.82	-1.72
			ResNet152	<b>60.19</b>	<b>70.92</b>	<b>43.62</b>	<b>34.43</b>	<b>14.13</b>	-1.71	-1.26	<b>17.23</b>	-3.47
ImageNet	$\ell_\infty$	Singh et al. (2023)	ConvNeXt-S-ConvStem	50.26	74.08	52.66	39.55	19.35	0.19	-0.42	26.87	1.14
			ConvNeXt-B-ConvStem	88.75	75.88	56.24	42.29	21.77	1.10	0.26	27.89	0.16
			ConvNeXt-L-ConvStem	<b>198.13</b>	<b>77.00</b>	<b>57.82</b>	<b>44.05</b>	<b>23.09</b>	<b>1.71</b>	<b>0.80</b>	<b>27.98</b>	-0.63

Table 8: The effect of different adversarial training methods on the OOD generalization of accuracy and robustness.

Dataset	Threat	Training	ID		OOD <sub>d</sub>				OOD <sub>t</sub>	
			Acc.	Rob.	Acc.	Rob.	EAcc.	ERob.	Rob.	ERob.
CIFAR10	$\ell_\infty$	PGD (Li & Spratling, 2023b)	<b>86.52</b>	<b>52.42</b>	<b>68.11</b>	31.55	-0.58	-0.61	26.47	-2.84
		VR- $\ell_\infty$ (Dai et al., 2022)	72.72	49.92	56.12	<b>31.84</b>	0.34	<b>1.47</b>	<b>34.70</b>	<b>6.55</b>
		PGD (Rice et al., 2020)	<b>85.34</b>	53.52	66.46	32.07	-1.12	-0.88	27.89	-1.94
		HE (Pang et al., 2020)	85.14	<b>53.84</b>	<b>66.96</b>	<b>32.45</b>	<b>-0.43</b>	<b>-0.72</b>	<b>46.20</b>	<b>16.22</b>
		PGD (locally-trained)	80.44	38.98	62.40	22.18	-0.60	-0.39	21.77	-1.27
		MMA (Ding et al., 2020)	<b>84.37</b>	<b>41.86</b>	<b>68.22</b>	<b>24.65</b>	<b>1.54</b>	<b>0.02</b>	<b>35.12</b>	<b>10.74</b>
		PGD Gowal et al. (2021a)	91.10	66.03	73.24	42.58	0.26	<b>0.71</b>	34.00	-1.67
		AS Bai et al. (2023)	<b>95.23</b>	<b>69.50</b>	<b>79.09</b>	<b>43.32</b>	<b>2.25</b>	-1.03	<b>46.71</b>	<b>9.41</b>

## G PLOTS OF CORRELATION PER DATASET SHIFT

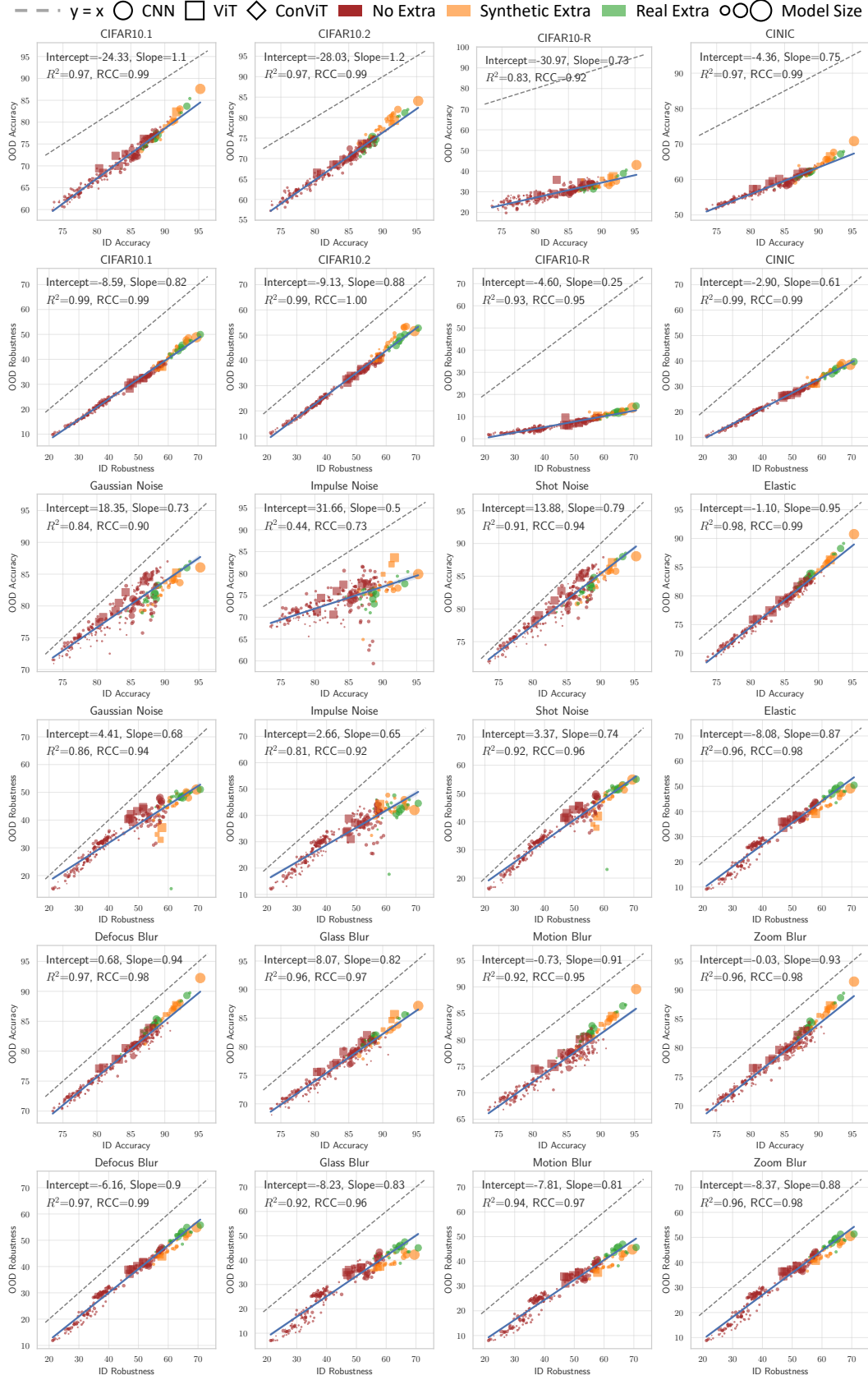


Figure 18: Correlation between ID accuracy and OOD accuracy (odd rows); ID robustness and OOD robustness (even rows) for CIFAR10  $\ell_\infty$  AT models



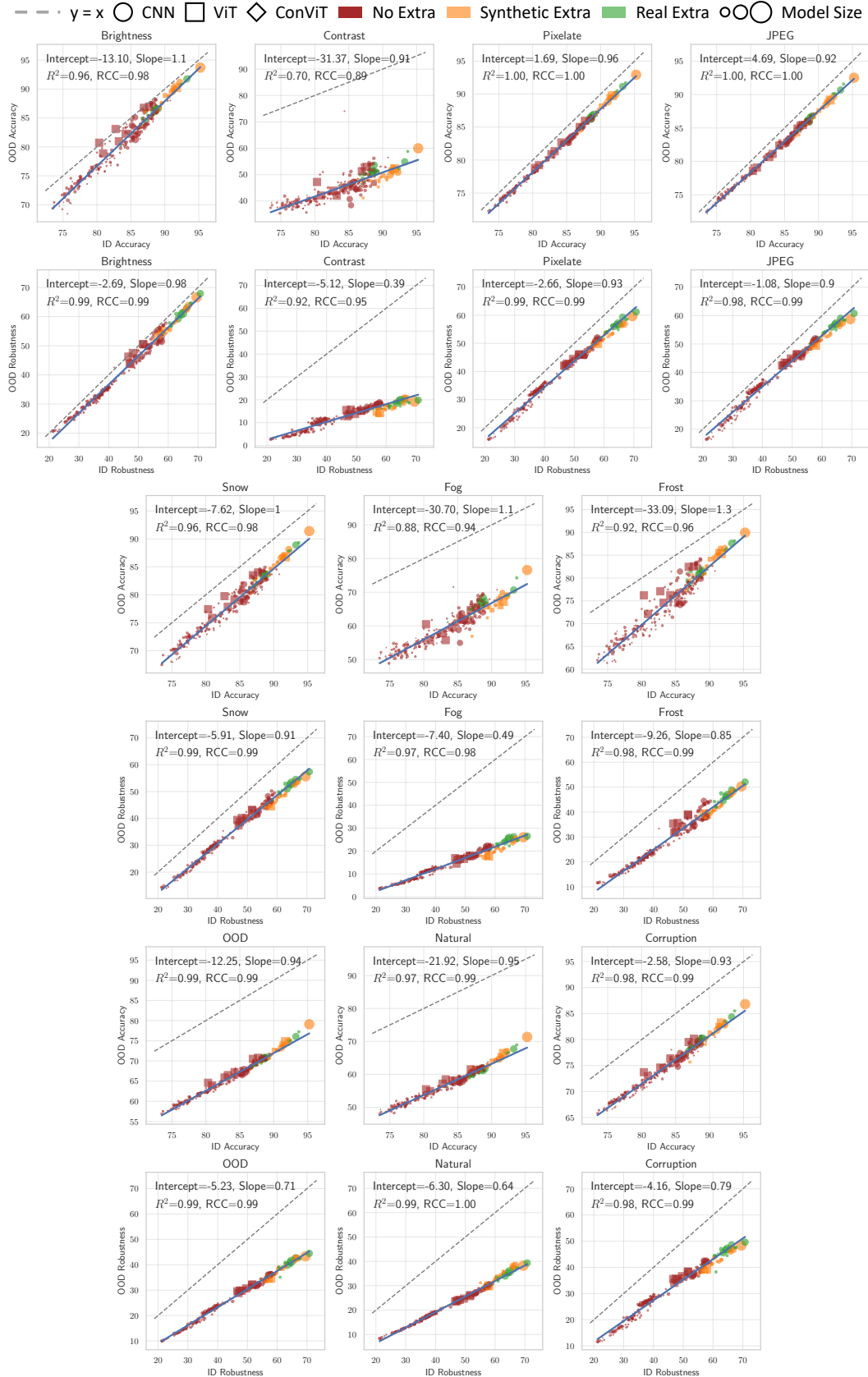
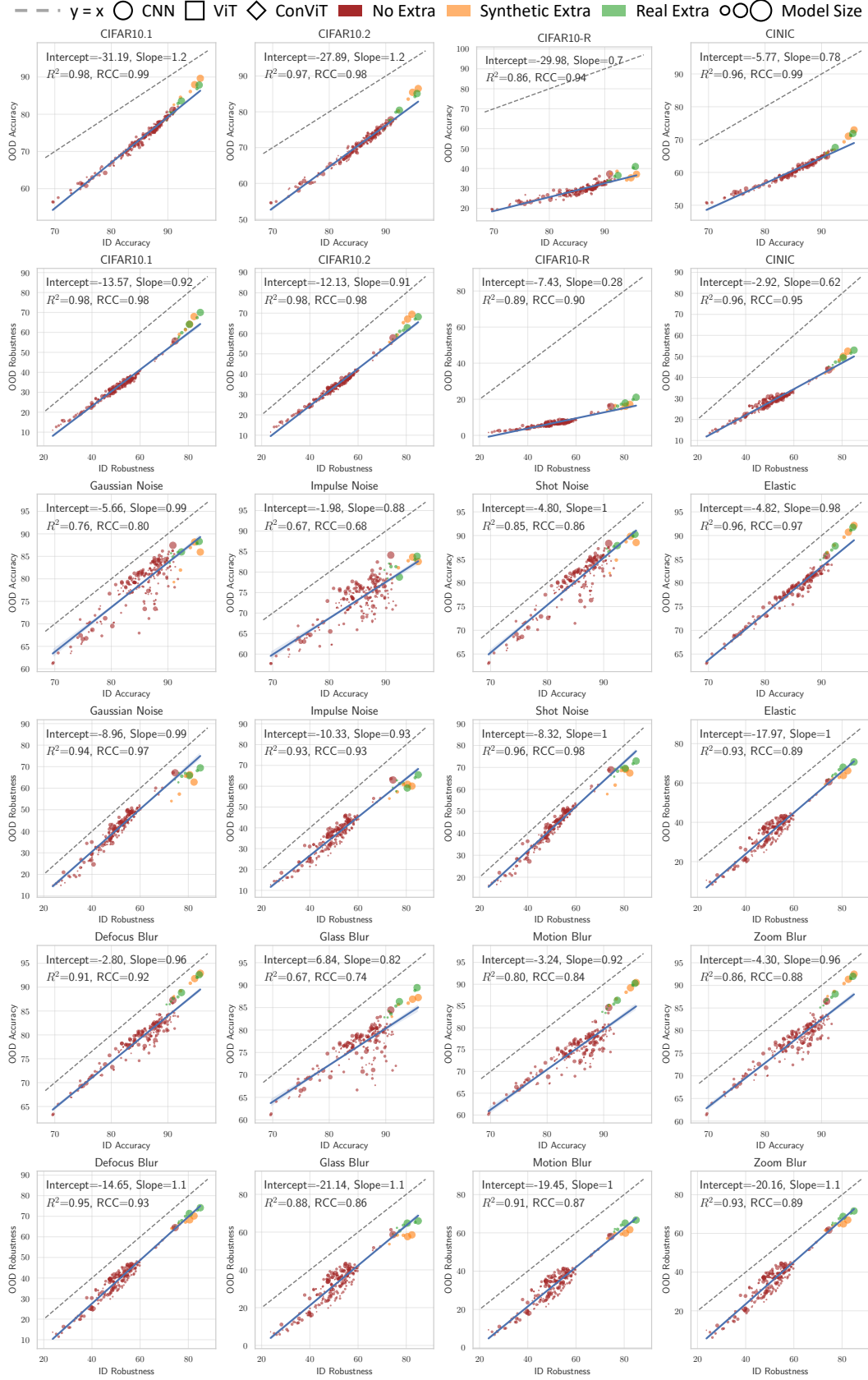
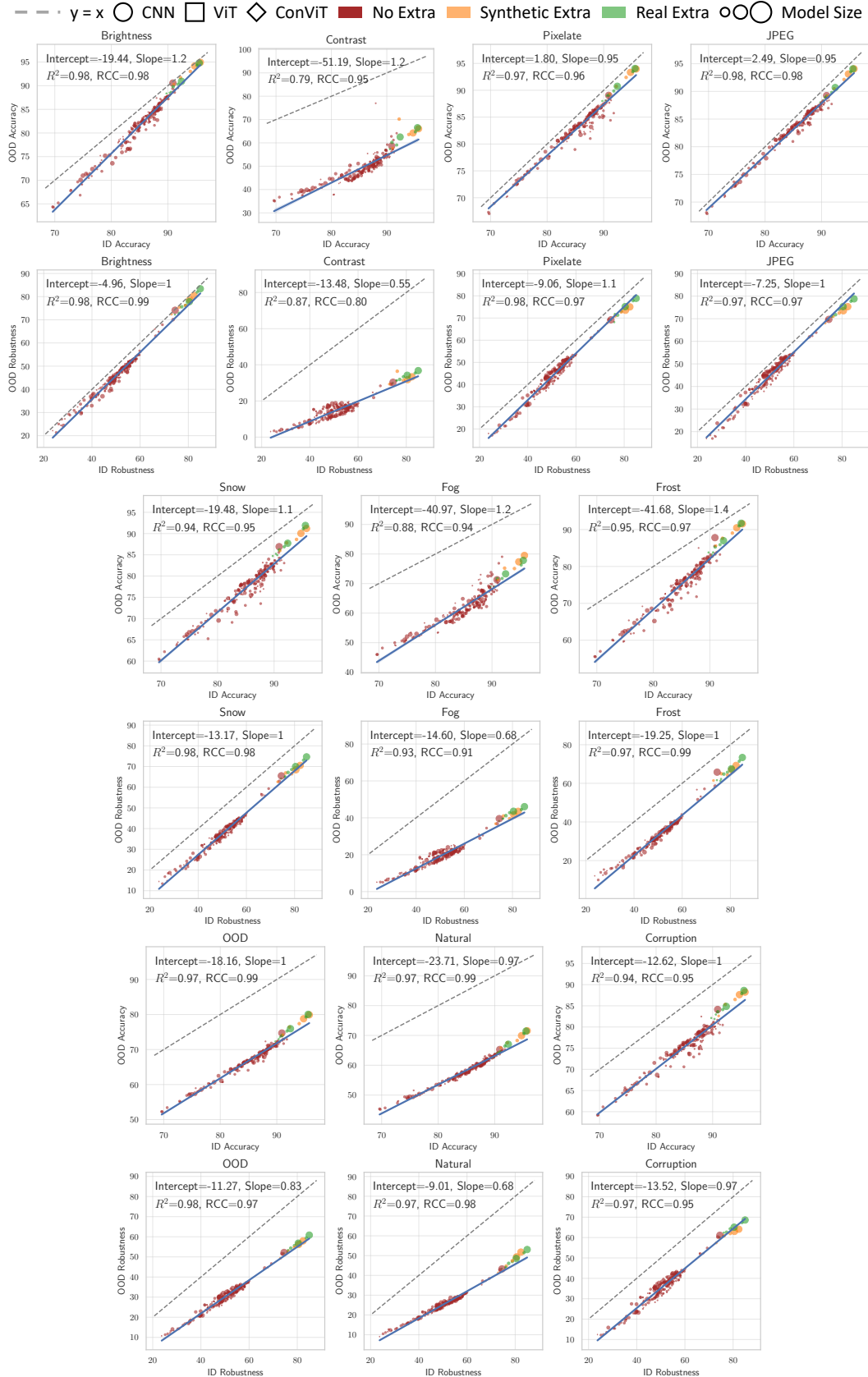


Figure 19: Correlation between ID accuracy and OOD accuracy (odd rows); ID robustness and OOD robustness (even rows) for CIFAR10  $\ell_\infty$  AT models

Figure 20: Correlation between ID accuracy and OOD accuracy (odd rows); ID robustness and OOD robustness (even rows) for CIFAR10  $\ell_2$  AT models



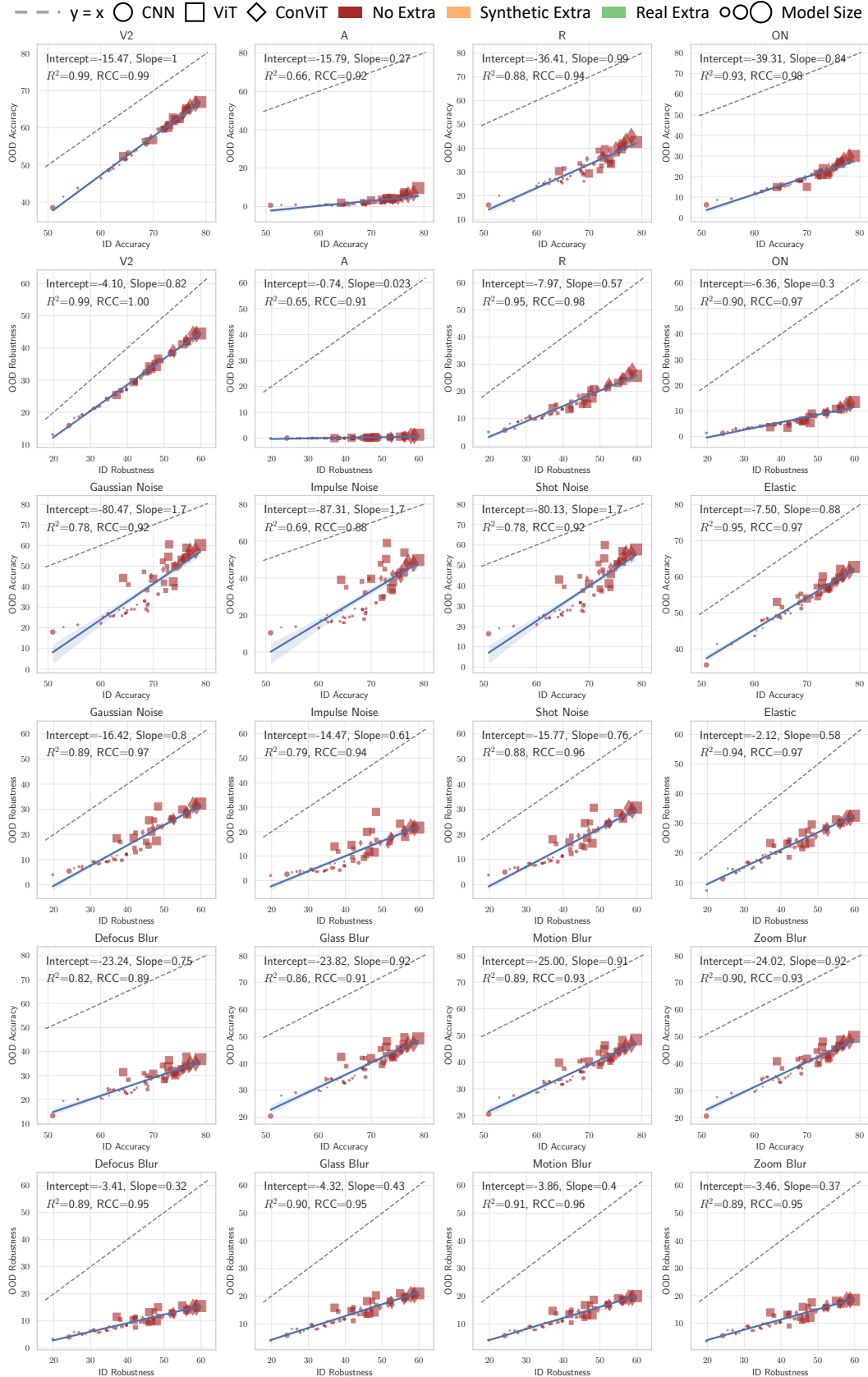


Figure 22: Correlation between ID accuracy and OOD accuracy (odd rows); ID robustness and OOD robustness (even rows) for ImageNet  $\ell_\infty$  AT models

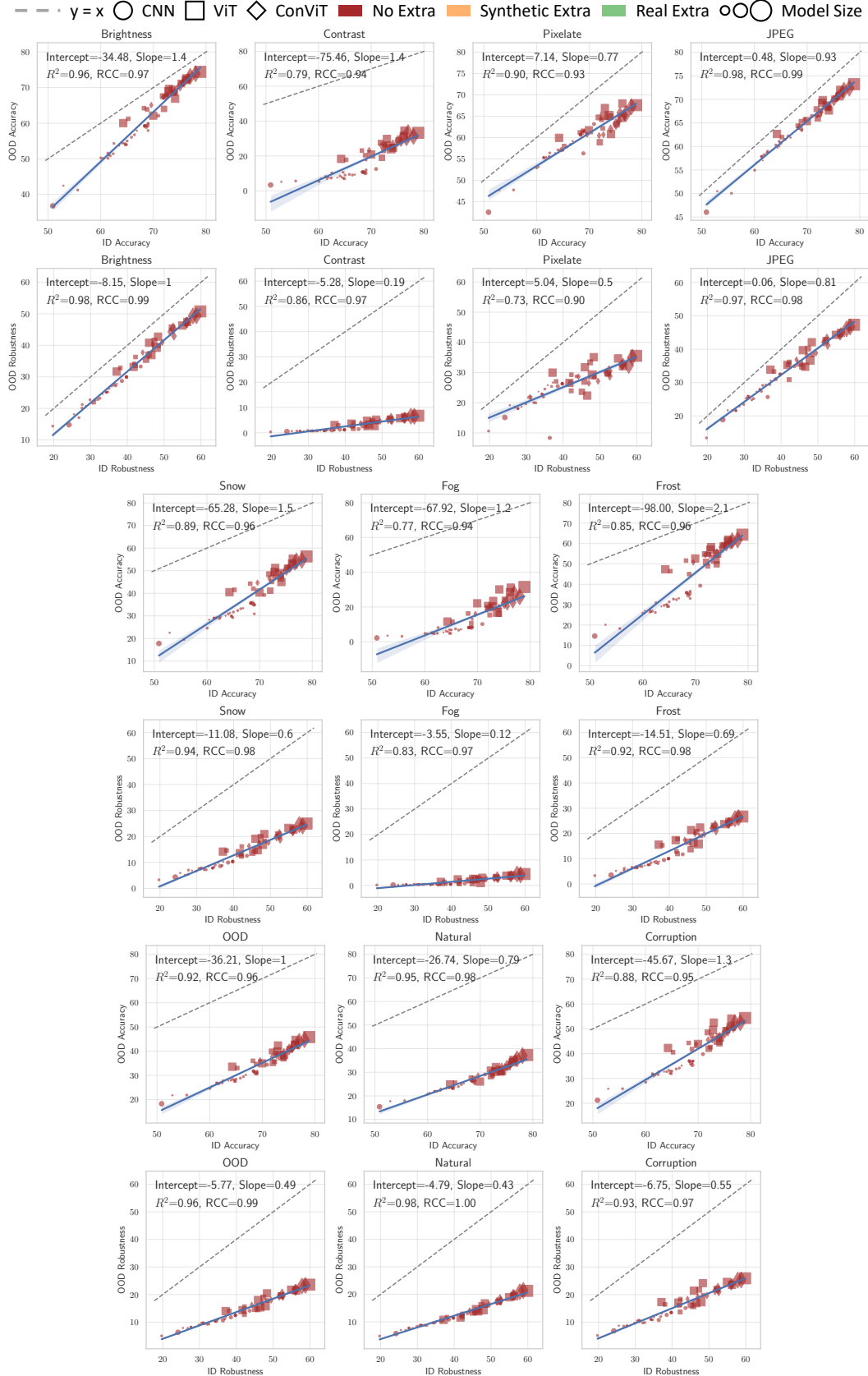


Figure 23: Correlation between ID accuracy and OOD accuracy (odd rows); ID robustness and OOD robustness (even rows) for ImageNet  $\ell_\infty$  AT models

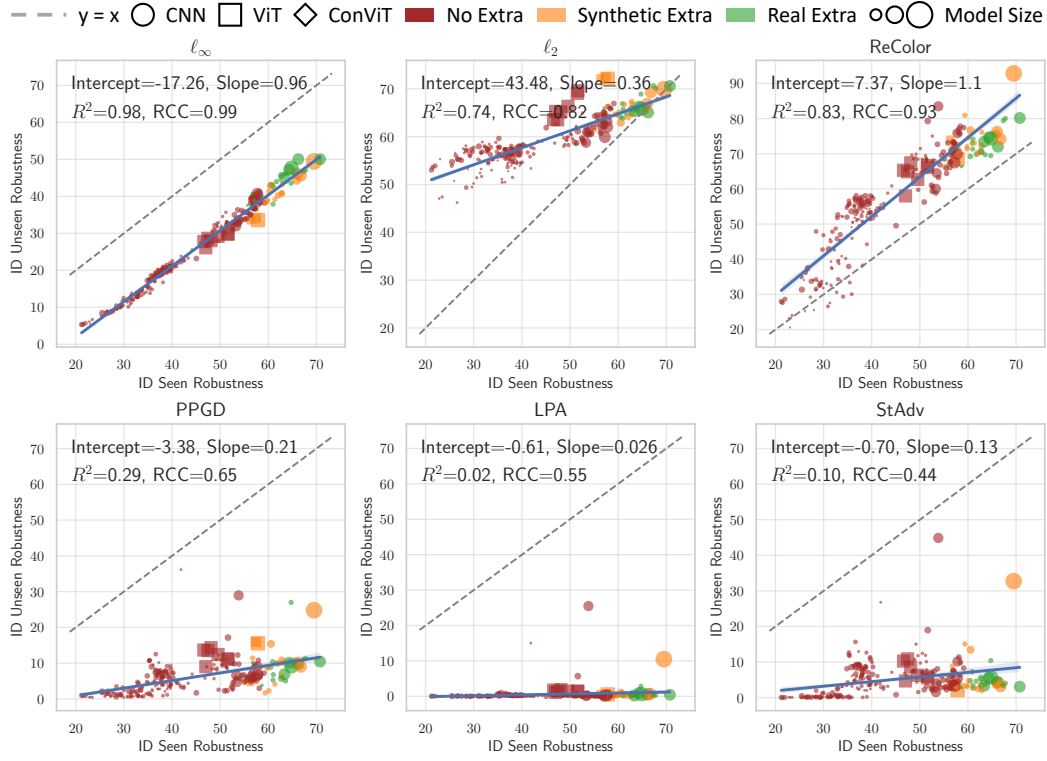
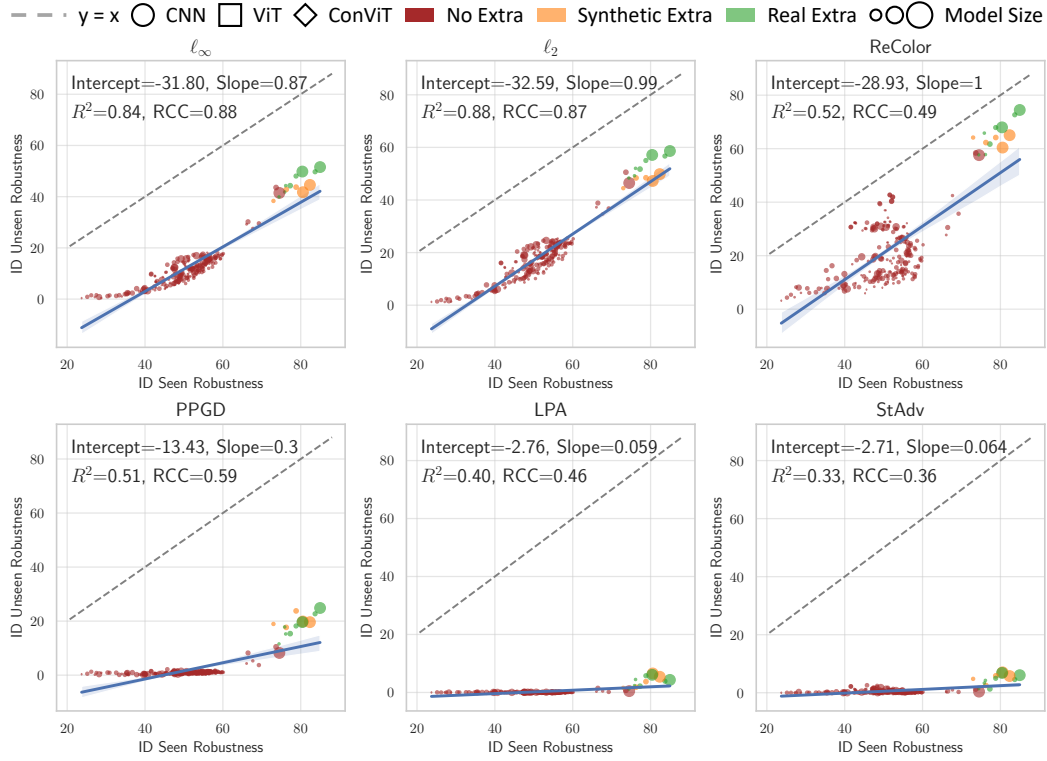
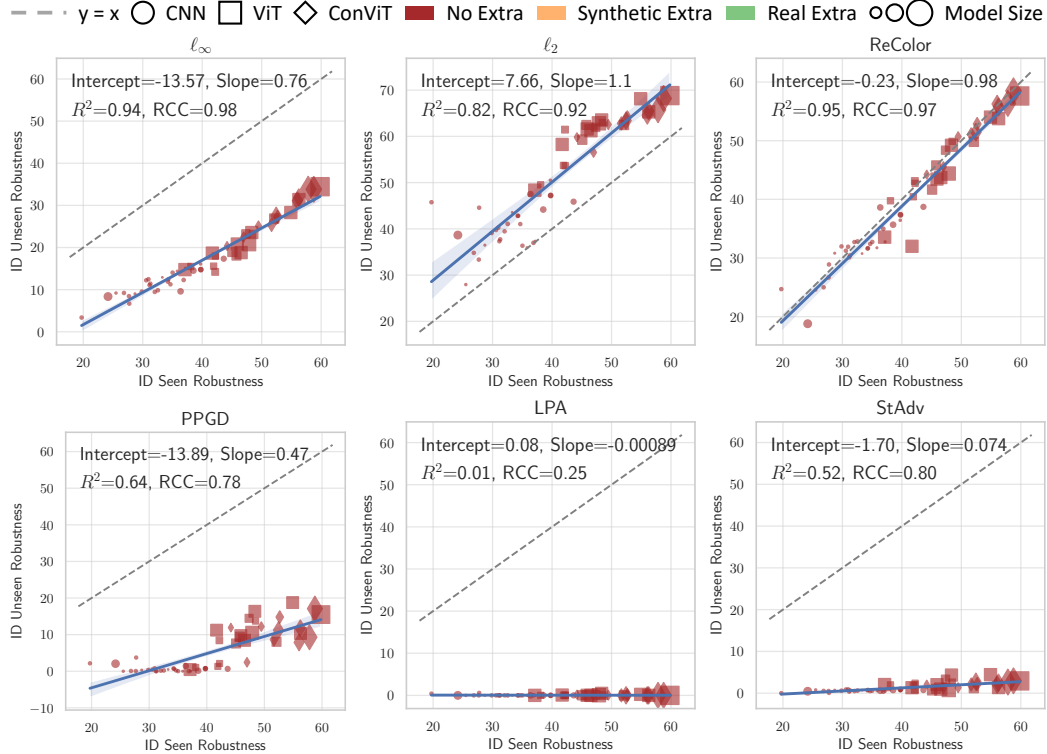


Figure 24: Correlation between seen and unforeseen robustness on ID data for CIFAR10  $\ell_\infty$  AT models

## H PLOTS OF CORRELATION PER THREAT SHIFT

Figure 25: Correlation between seen and unforeseen robustness on ID data for CIFAR10  $\ell_2$  AT modelsFigure 26: Correlation between seen and unforeseen robustness on ID data for ImageNet  $\ell_\infty$  AT models